

AD-762 481

TOTAL ELECTRON CONTENT STUDIES OF THE
IONOSPHERE

John A. Klobuchar, et al

Air Force Cambridge Research Laboratories
L. G. Hanscom Field, Massachusetts

1 February 1973

DISTRIBUTED BY:

NTIS

National Technical Information Service
U. S. DEPARTMENT OF COMMERCE
5285 Port Royal Road, Springfield Va. 22151

AFCL-TR-73-0098
1 FEBRUARY 1973
AIR FORCE SURVEY IN GEOPHYSICS, NO. 257

Handwritten initials

Handwritten circled number 1



AIR FORCE CAMBRIDGE RESEARCH LABORATORIES
L. G. HANSCOM FIELD, BEDFORD, MASSACHUSETTS

AD 762481

Total Electron Content Studies of the Ionosphere

JOHN A. KLOBUCHAR, et al

Reproduced by
NATIONAL TECHNICAL
INFORMATION SERVICE
U.S. Department of Commerce
Springfield VA 22151

Handwritten: DDC
RECEIVED
JUL 6 1973
RECEIVED
Handwritten: E

Approved for public release; distribution unlimited.

AIR FORCE SYSTEMS COMMAND
United States Air Force



Handwritten: 69

AFCL-TR-73-0098
1 FEBRUARY 1973
AIR FORCE SURVEY IN GEOPHYSICS, NO. 257



IONOSPHERIC PHYSICS LABORATORY PROJECT 4643

AIR FORCE CAMBRIDGE RESEARCH LABORATORIES

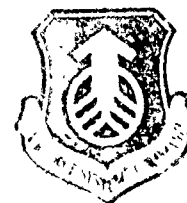
L. G. HANSCOM FIELD, BEDFORD, MASSACHUSETTS

Total Electron Content Studies of the Ionosphere

JOHN A. KLOBUCHAR, et al

Approved for public release; distribution unlimited.

AIR FORCE SYSTEMS COMMAND
United States Air Force



Unclassified
Security Classification

DOCUMENT CONTROL DATA - R&D		
<i>(Security classification of title, body of abstract and indexing annotation must be entered when the overall report is classified)</i>		
1. ORIGINATING ACTIVITY (Corporate author) Air Force Cambridge Research Laboratories (LI) L.G. Hanscom Field Bedford, Massachusetts 01730		2a. REPORT SECURITY CLASSIFICATION Unclassified
		2b. GROUP
3. REPORT TITLE TOTAL ELECTRON CONTENT STUDIES OF THE IONOSPHERE		
4. DESCRIPTIVE NOTES (Type of report and inclusive dates) Scientific, Interim.		
5. AUTHOR(S) (First name, middle initial, last name) John A. Klobuchar, et al		
6. REPORT DATE 1 February 1973	7a. TOTAL NO. OF PAGES 8769	7b. NO. OF REFS 42
8a. CONTRACT OR GRANT NO.		9a. ORIGINATOR'S REPORT NUMBER(S) AFCLR-TR-73-0098
a. PROJECT, TASK, WORK UNIT NOS. 4643-01-01		
c. DOD ELEMENT 62101F		
d. DOD SUBELEMENT 681000	9b. OTHER REPORT NO(S) (Any other numbers that may be assigned this report) AFSG No. 257	
10. DISTRIBUTION STATEMENT Approved for public release; distribution unlimited.		
11. SUPPLEMENTARY NOTES TECH, OTHER	12. SPONSORING MILITARY ACTIVITY Air Force Cambridge Research Laboratories (LI) L.G. Hanscom Field Bedford, Massachusetts 01730	
13. ABSTRACT Radio waves that pass through the earth's ionosphere travel more slowly than their free space velocity due to the group path delay of the ionosphere. This group path delay, directly proportional to the total electron content of the ionosphere, can be an important source of error to VHF, UHF and L-band satellite detection radars and satellite navigation systems. In this report, the current state of knowledge of ionospheric total electron content is outlined, with special emphasis placed on the North Atlantic region of the world due to NATO special requirements in this region. A numerical model of total electron content, valid over the European continent under certain conditions, is presented for systems engineering use for an average background total electron content correction. Typical values of total electron content are also given at various locations in the high, middle, and equatorial latitudes. If the results presented here seem incomplete, it is only because the state of knowledge of the total electron content parameter is still incomplete. With more observational data being taken at many locations, an over-all satisfactory picture of the world-wide behavior of this important parameter is beginning to emerge.		

DD FORM 1473
1 NOV 68

Unclassified
Security Classification

Unclassified

Security Classification

14. KEY WORDS	LINK A		LINK B		LINK C	
	ROLE	WT	ROLE	WT	ROLE	WT
Total electron content Equivalent slab thickness F region models						

Unclassified

Security Classification

Abstract

Radio waves that pass through the earth's ionosphere travel more slowly than their free space velocity due to the group path delay of the ionosphere. This group path delay, directly proportional to the total electron content of the ionosphere, can be an important source of error to VHF, UHF, and L-band satellite detection radars and satellite navigation systems. In this report, the current state of knowledge of ionospheric total electron content is outlined, with special emphasis placed on the North Atlantic region of the world due to NATO special requirements in this region. A numerical model of total electron content, valid over the European continent under certain conditions, is presented for systems engineering use for an average background total electron content correction. Typical values of total electron content are also given at various locations in the high, middle, and equatorial latitudes. If the results presented here seem incomplete, it is only because the state of knowledge of the total electron content parameter is still incomplete. With more observational data being taken at many locations, an over-all satisfactory picture of the world-wide behavior of this important parameter is beginning to emerge.

Contents

1. Introduction—Importance of the Total Electron Content Parameter, by John A. Klobuchar and Jules Aarons	1
2. TEC From the Faraday Effect, by John A. Klobuchar and Michael Mendillo	5
3. Total Electron Content Models, by John A. Klobuchar and Richard S. Allen	13
4. Available TEC and SLAB Thickness Data From S-66 Satellites, by John A. Klobuchar, John P. Mullen, and Douglas R. Seeman	19
5. A Numerical Model of TEC Over Europe for Sunspot Minimum Conditions, by John A. Klobuchar	27
6. A Comparison of TEC Obtained From Thomson Scatter and From Faraday Rotation, by John A. Klobuchar and Santi Basu	31
7. Data From the Three World Ionospheric Regions, by John A. Klobuchar and Douglas R. Seeman	35
8. Low Elevation Angle Measurements of Total Electron Content Taken From Thule, Greenland, by Michael Mendillo and John A. Klobuchar	55
9. Conclusions, by John A. Klobuchar	61

Illustrations

1-1.	Time Delay Due to the Ionosphere Versus Frequency for Several Values of Total Electron Content	3
1-2.	Multiplication Factor to Convert Vertical Electron Content to Slant Content for Various Choices of Mean Ionospheric Height	3
2-1.	Path of the Straight Line Ray From a Geostationary Satellite to Sagamore Hill, Hamilton, Massachusetts (42.6°N., 70.8°W)	8
2-2.	Polarization Twist (Ω , in Radians) and Total Electron Content (TEC, in el/m^2) Along the Slant Path From a Geostationary Satellite to a Mid-latitude Station	9
4-1.	Equivalent Slab Thickness for Various Stations for Winter and Summer Seasons	21
5-1.	Difference Between Model and Actual TEC (Units of $10^{16} \text{el}/\text{m}^2$)	29
5-2a.	Iso-contour of TEC Northern Europe as Reconstructed by the Numerical Model, Winter 1964-65	30
5-2b.	Original Iso-contour of TEC Over Northern Europe, Winter 1964-65	30
6-1.	A Comparison of Total Electron Content Obtained From the Faraday Effect and From Thomson Scatter	33
7-1.	Contour Maps of Total Electron Content for the Four Seasons of 1966 (BE-B and B-C)	36
7-2.	Total Electron Content for 1969 From the Panama Canal Zone	37

	Illustrations
7-3. Monthly Median Equivalent Slab Thickness for 1969 From the Panama Canal Zone	44
7-4. Total Electron Content From Kingston, Jamaica, West Indies, March 1972	44
7-5. A Comparison of Seasonal Median Values of Slab Thickness at Florence, Italy, and Hamilton, Massachusetts	45
7-6. A Comparison of Seasonal Median Values of Slab Thickness at Florence, Italy, and Hamilton, Massachusetts	45
7-7a. A Comparison of Monthly Median Slab Thickness at Aberystwyth, Wales, and Hamilton, Massachusetts	45
7-7b. A Comparison of Monthly Median Slab Thickness at Stanford, California, and Hamilton, Massachusetts	45
7-8. A Comparison of Monthly Median Slab Thickness at Stanford, California, and Hamilton, Massachusetts	46
7-9. Iso-Contours of Seasonal Median Total Electron Content Taken At Sagamore Hill, Hamilton, Massachusetts	47
7-10. Iso-Contours of Seasonal Median Total Electron Content Taken At Sagamore Hill, Hamilton, Massachusetts	48
7-11. Iso-Contours of Seasonal Median Total Electron Content Taken At Athens, Greece	49
7-12. Iso-Contours of Seasonal Median Total Electron Content Taken Over Northern Europe in 1965	50
7-13. Iso-Contours of Seasonal Median Total Electron Content Taken Over Northern Europe in 1966	51
7-14. Contours of Equivalent Slab Thickness Over Northern Europe - 1965	51
7-15a. Contour Map of Electron Content in a Geographic Latitude-LMT Plane for the Period 15/3-15/4/66 (After Bratteng and Frihagen, 1969)	52
7-15b. Contour Map of Electron Content in a Geographic Latitude-LMT Plane for the Period 15/10-15/11/65 (After Bratteng and Frihagen, 1969)	52
8-1. Sub-Ionospheric Latitude and M Factor vs Vertical Height From Thule Viewing ATS-3 Along the Station Meridian	56
8-2. Total Electron Content From ATS-3, Thule, Greenland, 1971 - Monthly Overplots of all Data	57
8-3. Total Electron Content From ATS-3, Thule, Greenland, 1971 - Monthly Medians	57
8-4. Total Electron Content From ATS-3, Thule, Greenland, During One Quiet and Two Disturbed Periods in April 1971	58
8-5. ATS-3 From Thule, Greenland, 14 and 25 April 1971	59

Tables

2-1.	Amount and Percent TEC Remaining Along Path to Satellite Above 10 deg Point and TEC and Q Above 1000 km Vertical Height	10
2-2.	Results of Computing M Using TEC to 1000 km, the 10 deg Point, and to the Geostationary Satellite Height	10
4-1.	Stations Where Slab Thickness Values Have Been Published	21
4-2.	Stations Where TEC Data May be Available	23
5-1.	Seasonal Coefficients Sets	28
5-2.	Seasonal Solar Flux	29
7-1-7-6.	Hourly Statistical Values of Total Electron Content and Equivalent Slab Thickness From Hamilton, Massachusetts	38

Contents

1-1	Introduction	1
1-2	Some Comments on the Existing Data Base	3
	References	4

TOTAL ELECTRON CONTENT STUDIES OF THE IONOSPHERE

1. Introduction - Importance of the Total Electron Content Parameter

J.A. Klobuchar and J. Aarons

1-1. INTRODUCTION

The total electron content (TEC) of the earth's ionosphere is defined as the total number of free, thermal electrons in a unit area column of ionosphere from the ground to a height well above the peak of ionization, to at least 1000 km. This TEC is usually described as a vertical column one square meter in area. Typical TEC values range from 10^{16} to 10^{19} el/m², but the exact value is a function of many variables. Some of the variables which influence TEC are geographic location, local time, season, solar EUV flux, and magnetic activity. In a given day at one location, changes in TEC of 10 to 1, or greater, are typical in some seasons.

Why is the TEC parameter studied? What importance does it have? First, experimentally it has been a relatively simple parameter to measure. The earliest TEC results, obtained in the late 1950s, showed the first temporal and seasonal behavior of the topside of the ionosphere. Comparisons were later made of the ratio of the topside to the bottomside content. The equivalent slab thickness, the ratio of TEC divided by the density at the peak of the F-region, also was studied. Slab thickness is the equivalent thickness the ionosphere would have if it had a constant density equal to the peak density throughout its entire height. The slab thickness generally ranges from 100 to 400 km in height.

(Received for publication 7 February 1973)

The chief scientific value of TEC today lies in its simplicity of measurement, providing a suitable satellite source is available. TEC provides continuity of F-region measurements through magnetically disturbed periods. TEC measurements have the potential use as another routine parameter describing the F2 region at many locations.

What engineering importance does TEC have? Any operating or potential system which involves radio waves propagating through the ionosphere and which requires time delay measurements to an accuracy of the same order as the ionosphere time delay errors requires a knowledge of TEC to correct for these errors. The ionosphere produces a retardation in the velocity of the information carried on a radio wave called group path delay. This group path delay produces timing errors in radar systems and navigation systems which must traverse the ionosphere. The group path delay timing error is directly proportional to the TEC.

The group path delay timing error can be important depending upon the frequency the system uses and the amount of the ionospheric TEC. For VHF and higher the relationship between time delay Δt and TEC is:

$$\Delta t = \frac{40.3}{c f^2} \text{ TEC (sec)}$$

where

c = velocity of light = 3×10^8 m/sec

f = system operating frequency in Hz

TEC = total electron content in el/m^2

A typical time delay for a radar operating at 430 MHz might range from 10 to 1000 nsec for a target at the zenith. Figure 1-1 shows a plot of time delay versus frequency for several TEC values. At 25 deg elevation these time delays would be approximately doubled due to the greater TEC encountered through an oblique ionospheric path. Figure 1-2 shows the factor by which vertical TEC values must be multiplied to obtain TEC time delay values at other elevation angles. Typical mean ionospheric heights range from 300 to 400 km for this conversion ratio. This does not, of course, correct for temporal or geographic gradients of TEC which produce an additional difference between vertical and oblique TEC values.

In order to determine the time delay correction for an object at an arbitrary height, geographic location and time in the ionosphere, a complete description of the electron density height profile for all times and locations must be known. This task is well beyond the scope of this report. Here, only the status of measurements of TEC, the total vertically integrated electron density up to a height of at least 1000 km, will be discussed. First, some comments will be made on the existing TEC data base, along with prospects for improving this data base. Next, the approximations which are a part of the TEC data base will be discussed. These

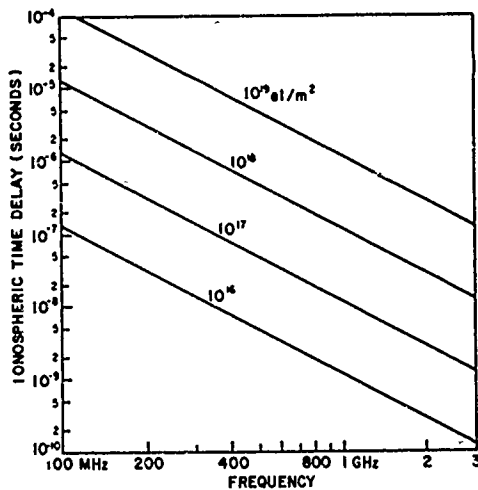


Figure 1-1. Time Delay Due to the Ionosphere Versus Frequency for Several Values of Total Electron Content

with a discussion of TEC data obtained from the three world ionospheric regions—the equatorial, midlatitude, and polar regions. A brief summary discusses possible improvements in TEC prediction capability in the near term, ultimate limitations to TEC data and possible experimental work which will improve TEC prediction accuracy.

1-2. SOME COMMENTS ON THE EXISTING DATA BASE

Measurements of the total electron content of the ionosphere have been made since the late 1950s. The earliest measurements were made by monitoring the polarization twist of vhf lunar reflected radio waves. Following the advent of artificial earth satellites the Faraday polarization rotation and differential Doppler effects were used to determine TEC from VHF radio waves transmitted from certain satellites. The differential Doppler and differential Faraday effects have also been used to determine the height profile of electron density by means of rocket probes.

Numerous ionospheric observatories participate in taking TEC data from one or more artificial earth satellites but little has been done to integrate the results from the various independent observers and to attempt to produce a world-wide picture of ionospheric total electron content from the measurements taken from these satellites. In fact, it may not be possible to compile an over-all picture of TEC from these data as the available data from many of these stations consists of the results of a few satellite passes a day averaged over a few month period. These seasonal averages were compiled using different times and lengths of seasons for

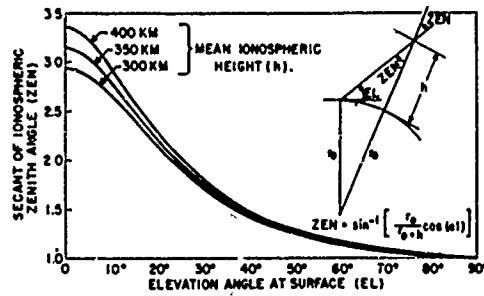


Figure 1-2. Multiplication Factor to Convert Vertical Electron Content to Slant Content for Various Choices of Mean Ionospheric Height

sections will be followed by a brief description of efforts to date in TEC modelling. Finally, in the data section, tables and graphs of TEC averages for several locations are presented along

the various observers. As a result, combining these seasonal averages from the various stations encounters the difficulty that even the mean seasonal picture may suffer from these sampling differences. No day to day variability can be determined from the mean seasonal data.

One exception to the rather bleak picture of the state of the available TEC data obtained from low orbit satellites is in the European continent where Amayenc, Bertin and Papet-Lepine (1971) combined TEC data from near Paris, France, with that of Liszka's (1967) data taken at Kiruna, Sweden, to produce mean seasonal maps of TEC various local mean time from 39 to 72 deg North latitude. These TEC contours, graciously supplied by F. Bertin for inclusion in this report, are included in the data section.

Geostationary satellite polarization data are much better with regard to data time sampling, but, unfortunately, the geographic distribution of the available data is severely restricted by the lack of geostationary satellites having suitable VHF transmissions. Most of the available total electron content data from geostationary satellites have been taken from the North American continent and from the Australia-New Zealand area, with data also available from Japan, Hawaii, and Wales. The European continent, until late 1971, has not had a suitable geostationary satellite available for long periods of time to make ionospheric measurements.

Perhaps the main point concerning availability of TEC data is that there is not now - nor is there likely to be in the near future - sufficient TEC data from a large enough number of stations to construct a world-wide TEC model directly from TEC data alone. Therefore, any TEC model, except one which covers only a limited geographic region, must lean heavily on other existing models of the F2 region. A world-wide foF2 prediction model was made using data from more than 50 ionosondes for the sunspot minimum conditions and from over 100 ionosondes during the International Year sunspot maximum. Direct TEC measurements have little hope of being available from this number of stations. Therefore, models of TEC must necessarily rely heavily on existing foF2 data maps.

References

- Amayenc, P., Bertin, F., and Papet-Lepine, J. (1971) Sur l'evolution latitudinal du contenu electronique de l'ionosphere, Annales de Geophysique, 27:(No. 3, 345-357.)
- Liszka, L., (1967) The high-latitude trough in ionospheric electron content, J. Atmos. Terr. Phys., 29: 1243-1259.

Contents

2-1	Introduction	5
2-2	The Faraday Method of TEC Measurements	5
2-3	Absolute Accuracy of Measurements of Polarization Rotation	7
2-4	Model Calculations-Assumptions and Data Used	8
2-5	Model Calculations-Exospheric Contribution to the TEC	9
2-6	Discussion	10
2-7	Determining Diurnal in Mean Flight Height	11
	Acknowledgments	11
	References	12

2. TEC From the Faraday Effect

J.A. Klobuchar and M. Mendillo

2.1. INTRODUCTION

Measurements of the ionospheric total electron content (TEC) are being made at several mid-latitude sites by monitoring the Faraday rotation of VHF radio waves from geostationary satellites. The correct conversion of the polarization data to equivalent vertical TEC values is mainly dependent upon the choice of the \bar{M} factor which appears in the Faraday equation. A recent paper by Smith (1970) concludes that large errors may result if a constant \bar{M} factor is used throughout the course of a day. Here we present the results of calculations made of the total Faraday rotation and the "true" number of electrons along a path from a mid-latitude station to a geostationary satellite. Typical summer and winter, day and night conditions were used to determine how the \bar{M} factor, the polarization twist (Ω) and the TEC change as a function of height.

2.2. THE FARADAY METHOD OF TEC MEASUREMENTS

The amount of total polarization twist, Ω , is related to the total electron content by the well known relation:

$$\Omega = \frac{K}{f^2} \int B \cos \theta \sec X N dh \quad (\text{radians}) \quad (2-1)$$

where:

$$K = 2.36 \times 10^{-5}$$

f = frequency in Hertz

B = magnetic field strength in gammas

θ = propagation angle

χ = zenith angle

N = local electron density in el/M^2 .

In practice, the measured amount of polarization twist, Ω , is converted to an equivalent total vertical electron content by removing $B \cos \theta \sec \chi$ from under the integral sign and replacing it with a mean value. Then:

$$\Omega = \frac{K}{f^2} \overline{B \cos \theta \sec \chi} \int N \, dh \quad (2-2)$$

where $\overline{B \cos \theta \sec \chi} = \overline{M}$ is computed in the following manner. A typical $N(h)$ profile is assumed and calculations of the mean value \overline{M} are generally found by equating:

$$M = \frac{\int B \cos \theta \sec \chi N \, dh}{\int N \, dh} \quad (2-3)$$

The crux of this discussion lies in the limits of the integration in both the numerator and the denominator in Eq. (2-3). At least one author, Smith (1970), has pointed out that there is a large diurnal change in \overline{M} when polarization observations are made from signals transmitted from a geostationary satellite. He used $N(h)$ from the Thomson scatter facility at Arecibo to heights of ≈ 1000 km, the Angerami and Thomas (1964) exospheric electron density model above that height, and integration limits from the ground to the satellites in order to determine the diurnal changes in \overline{M} .

In the calculations which follow we will show that an \overline{M} derived from Eq. (2-3) is in error if the integration is carried out to the satellite height. The integration of both the numerator and the denominator in Eq. (2-3) should only be carried out to heights where Ω is no longer measurable. If this point is ignored, the resultant $\int N \, dh$ will consist of both the TEC actually responsible for the measured amount of rotation (Ω), plus an additional $\int N \, dh$ along the ray path where a nonmeasurable amount of rotation occurs. In summary, then, Eq. (2-3) should be rewritten, using Eq. (2-1) to read:

$$\overline{M} = \frac{f^2}{K} \frac{\Omega}{\int N \, dh} \quad (2-4)$$

where Q is the measured amount of rotation, and the upper limit to the integral corresponds to the height above which the remaining amount of rotation is less than the absolute experimental error.

2.3. ABSOLUTE ACCURACY OF MEASUREMENTS OF POLARIZATION ROTATION

Before the results of the calculations of Q and TEC are presented a discussion of the absolute measurement accuracy of the experimental quantity in the Faraday technique, (Q) is in order. Measurements of the polarization twist of VHF radio waves from geostationary satellites are usually carried out by means of rotating or spinning yagis. The position of the null in the arriving signal plane is compared either mechanically or electrically with some reference polarization; for example, the local vertical. Some workers use a pair of right hand and left hand circularly polarized helices, with a dual phase locked receiver, and compare the phase difference at the two receiver outputs. The simple yagi or helical antennas generally used to measure the relative polarization with respect to a local reference can determine this angle on a relative basis to within approximately ± 5 deg, if careful calibration of the receiving system is carried out and maintained.

A correction also must be made for the angle that the transmitted signal from the satellite would make with respect to the local vertical in the absence of an ionosphere. The orientation that the transmitted VHF wave makes with respect to the satellite spin axis, or to some known reference, is usually not known precisely, since measurements of this transmitted orientation are not made before launch. Consequently, resort must be made to calculations of this angle based upon the satellite VHF antenna and feed characteristics. In the case of ATS-3, an independent determination of this angle was made by measuring the total twist of lunar reflected signals at a high VHF frequency at a time when the moon was nearly directly behind the ATS-3 satellite, Klobuchar (1969). By knowing the absolute amount of twist on the lunar reflected signal and relative amount of measured twist along the ATS-3 path, the transmitted polarization of the VHF signal on the ATS-3 was determined. The accuracy of either the calculated or the experimental methods of determining this transmitted polarization is certainly no better than ± 5 deg. In addition the satellite spin axis may have some diurnal precession of a few degrees about the nominal polar axis. In conclusion, we estimate the total polarization twist measurement error due to all sources, at least for the modest antennas used by most workers, to be not better than ± 10 deg.

2-4. MODEL CALCULATIONS-ASSUMPTIONS AND DATA USED

In order to see how Ω and $\int N dh$ vary as a function of height along the path toward a geostationary satellite, we carried out integration of Ω and N from a mid-latitude station at Hamilton, Massachusetts, (42.6°N , 70.8°W) to a geostationary satellite on the station's meridian. We used $N(h)$ data up to a vertical height of 1000 km, obtained from the Thomson scatter radar at Millstone Hill, kindly provided by J. V. Evans of the MIT Lincoln Laboratory. $N(h)$, above a vertical height of 1000 km, was derived from the Angerami and Thomas (1964), (A&T) diffusive equilibrium exospheric model. The calculations of polarization twist and TEC as a function of height along the straight line path from the satellite to the station were made for four conditions, summer and winter day and night.

To calculate the electron density at some point along a field line the A&T exospheric model requires a temperature, composition, and electron density at the base of the exosphere along the same field line, here taken as 1000 km. In order to compute the electron density along the straight line path to the satellite these

parameters are required for the A&T model over a substantial latitude range. Figure 2-1 shows that the minimum L reached by a ray from Hamilton, Massachusetts, to the geostationary satellite on the station meridian is $L = 2.3$, which corresponds to an invariant latitude at 1000 km (Λ') of 44 deg. $L = 4.6$ ($\Lambda' = 60$ deg) is taken as the plasmapause outside of which we take a constant electron density of 200 el/cm^3 .

The electron density at the 1000 km base level of the exosphere at the latitude of Millstone Hill ($\Lambda' = 55$ deg) is taken from the Thomson scatter profiles provided by Evans. The electron density over the

remainder of the 44 to 60 deg latitude range is taken from the gradients given by Brace, Mayr and Reddy (1967) fitted to the Millstone Hill values at 55 deg.

Electron temperatures over the same latitude range were obtained by using the temperature gradients of Brace et al, fitted to the actual T_e values measured at 1000 km at Millstone Hill, also kindly provided by Evans. In the A&T model of diffusion along a field line the ion and electron temperatures are assumed to be equal to the 1000 km value. Ion composition was chosen on the basis of measured

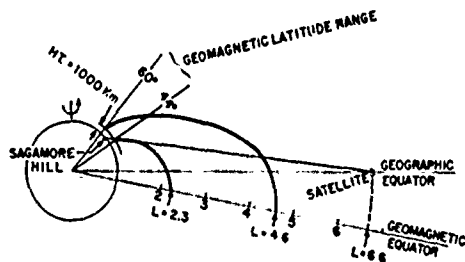


Figure 2-1. Path of the Straight Line Ray From a Geostationary Satellite to Sagamore Hill, Hamilton, Massachusetts (42.6°N , 70.8°W). The satellite is on the station meridian

values at Arecibo ($\Delta' = 33$ deg), Prasad (1970), and estimated values at 55 deg fitted with a linear change between these two latitudes.

2.5. MODEL CALCULATIONS-EXOSPHERIC CONTRIBUTION TO THE TEC

Results of the calculations of Q and TEC from the satellite to the station for the four cases being considered are shown in Figure 2-2. Both Q and TEC above the ordinate height are plotted as a function of height. The values above 1000 km

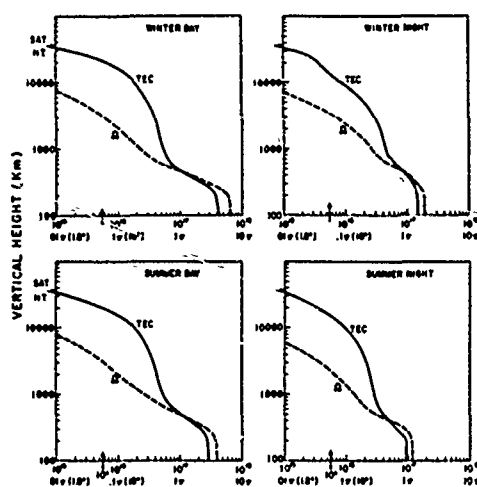


Figure 2-2. Polarization Twist (Q , in Radians) and Total Electron Content (TEC, in $e1/m^2$) Along the Slant Path From a Geostationary Satellite to a Mid-Latitude Station

in vertical height, shown in Figure 2-2, are from the A&T model calculations. Below 1000 km Q and TEC are from Evans' $N_e(h)$ profiles. All values were computed along the slant path at 41 deg elevation angle, though the ordinate is the more commonly used vertical height. The point where 10 deg of rotation occurs, which is within the estimated error of measurement accuracy of most observers, is indicated on the abscissa by a small arrow. Note that above this point, where only 10 deg of rotation remains, there is still a significant TEC. Table 2-1 indicates both the amount and the percent TEC remaining along the path to the satellite above the 10 deg point, and the TEC above 1000 km vertical height.

As Table 2-1 shows, there is still a significant percentage of TEC above the point where the remaining Faraday rotation is within the measurement error. Hence, the Faraday rotation effect does not respond measurably to this portion of the "true" total electron content.

Table 2-2 gives the results of computing \bar{M} according to Eq. (2-4), including both Q and TEC up to three heights; 1000 km, the point above which the remaining rotation is less than 10 deg, and, the satellite height. Also shown in Table 2-2 are the percentage changes for each condition from a mean of the four cases.

The results in Table 2-2 show that the day to night change in the \bar{M} factor is smallest for \bar{M} derived by using Q and TEC up to 1000 km. If \bar{M} is obtained by choosing the integration limits in Eq. (2-4) at the height of 10 deg of remaining rotation the day to night change is still rather small. The worst case is in winter,

Table 2-1. Amount and Percent TEC Remaining Along Path to Satellite Above 10 deg Point and TEC and Ω Above 1000 km Vertical Height

	TEC above 1000 km	% TEC above 1000 km	Ω above 1000 km	% Ω above 1000 km	TEC above 10 deg point	% TEC above 10 deg point
Winter Day	5.19	12.2	40°	3.4	3.72	8.8
Winter Night	4.53	30.8	47°	13.7	2.73	18.6
Summer Day	5.35	18.6	51°	6.9	3.56	12.4
Summer Night	2.91	31.3	25°	11.6	2.34	25.4

Table 2-2. Results of Computing \bar{M} According to Eq. (2-4)

	\bar{M}_{1000}	\bar{M}_{100}	\bar{M}_{total}	\bar{M}_{1000}	$\bar{M}_{10\text{ deg}}$	\bar{M}_{total}
				(Percent Changes)		
Winter Day	60236	59251	52906	2.9	4.6	13.9
Winter Night	57062	53434	42508	-2.5	-5.6	-8.5
Summer Day	58353	56934	48577	-0.3	-0.5	4.6
Summer Night	58475	56908	41854	0	0.5	-9.9

where a 10 percent day to night error is calculated. However, if \bar{M} is calculated using integration limits to the height of the satellite, the day to night \bar{M} change is 22.4 deg in winter and 14.5 deg in summer. The mean \bar{M} is 18 percent less than the \bar{M} calculated to the 10 deg point and 20.6 percent less than \bar{M} computed using integration limits of 1000 km. The difference between the mean \bar{M} for 1000 km and for the 10 deg height point, however, is only 3.2 percent.

2.6. DISCUSSION

We have shown examples of four cases of calculations of Ω and TEC calculated up to a geostationary satellite from a mid-latitude station. The four cases were chosen to represent ionospheric diurnal maximum and minimum conditions where the contribution from the exosphere might be expected to be a minimum and a maximum of the total TEC respectively. The A&T model used is a constant temperature model along field lines and requires a knowledge of temperature, composition and electron density at the base level over a 44 to 60 deg latitude range. Because of the several parameters of the model, which itself is an approximation, these calculations may not reflect the actual exospheric densities. They do show, however, that the polarization twist predominantly occurs in the ionosphere, with only from 3 to 14 percent occurring above 1000 km.

In summary, the Faraday technique, when used with VHF signals transmitted from geostationary satellites, remains a good measure of the ionospheric total electron content; but it is not a satisfactory measure of the exospheric electron content. Changing the \bar{M} factor in an attempt to account for the electrons above the point where they are measured by the Faraday effect is misleading, we believe, and can be in serious error. We maintain that a more-satisfactory method of presenting TEC results obtained from VHF signals from geostationary satellites is to use an \bar{M} factor calculated by using typical profiles up to a standard height of 1000 km and to include any exospheric TEC contribution as an additive constant.

2.7. DETERMINING DIURNAL IN MEAN FIELD HEIGHT

After this section of the report was written, a paper by J. E. Titheridge (1972) was published in which he used a wide range of model ionospheres and satellite and station locations to determine diurnal changes in the mean field height. He concluded that a fixed mean height of 420 km gives a resultant accuracy of plus and minus 5 percent in TEC up to a mean height of approximately 2000 km under most conditions. Our work is in agreement with his conclusions, which are more general in geographic coverage.

Another point concerning the conversion of the Faraday polarization twist to TEC has been raised by R. Fritz (private communication). He pointed out that the diurnal change in position of a geostationary satellite due to a non-zero orbital inclination can produce a change in the mean \bar{M} factor, even at the constant mean height, of plus and minus 5 percent. A knowledge of the precise orbit of the satellite can be used to correct for this error.

Acknowledgments

We gratefully acknowledge the electron density and temperature data given us by J. V. Evans, MIT Lincoln Laboratory, for use in this study.

References

- Angerami, J. J., and Thomas, J. O. (1964) Studies of Planetary Atmospheres, (1) The distribution of electrons and ions in the earth's exosphere, J. Geophys. Res. 69:4537-4560.
- Brace, L. H., Mayr, H. G., and Reddy, B. M. (1968) The early effects of increasing solar activity upon the temperature and density of the 1000 kilometer ionosphere, J. Geophys. Res., 73:1607-1615.
- Klobuchar, J. A. (1969) Polarization angle of VHF telemetry transmitters on ATS-3, ATS Technical Data Report, Goddard Space Flight Center, Greenbelt, Maryland.
- Prasad, S. S. (1970) Ionic composition and temperature over Arecibo 2, J. Geophys. Res. 75:1911-1918.
- Smith, D. H. (1970) Diurnal variation of the mean Faraday factor at Arecibo, J. Geophys. Res., 75:823-828.
- Titheridge, J. E. (1972) Determination of ionospheric electron content from the Faraday rotation of geostationary satellite signals, Planet. Space Sci., 20:353-369.

Contents

3-1	The ESSA-NOAA Ionospheric Profile Model	13
3-2	The AFCRL First Order Mid-Latitude TEC Model	14
3-3	SAMSO Studies	14
3-4	NASA-DBA Studies	15
3-5	Comments on Model Studies	15
3-6	The Pennsylvania State Mark I Model	16
3-7	Limitations of Present Model Studies	16
3-8	Advantages of Combined TEC and SLAB Thickness Model	16
	References	17

3. Total Electron Content Models

J.A. Klobuchar and R.S. Allen

Recently there has been much interest by systems engineering groups and by other non-ionospheric workers in the time delay caused by the number of free electrons in the earth's ionosphere. These groups include those who require error correction for UHF radars, proposed geostationary satellite navigation systems, satellite tracking stations using VHF beacons, and radio astronomers who are attempting to measure accurate positions and distances by means of very long baseline interferometry. As a result of all this interest several models of TEC-time delay have been made by different groups. Most of these models have been constructed using a limited data base, hence, the applicability both in geographical extent and in time in the solar cycle is limited. A brief outline of these models is presented below.

3-1 THE ESSA-NOAA IONOSPHERIC PROFILE MODEL

The Environmental Science Services Administration [Wright, (1967)], does true height analysis of ground based ionosondes to find the electron density up to the peak of the F2 region. Above the peak they use the following expression:

$$N = N_{\max} \cdot \exp \frac{1}{2} \left\{ (1 + g) \cdot (1 - z - e^{-z}) \right\}$$

where

$$z = \frac{1}{g} \ln \left[1 + g \frac{(h - h_{\max})}{H} \right] \quad \begin{array}{l} g = 0.05 \\ H = \text{scale height.} \end{array}$$

This resulting profile is accurate up to the peak of the F2 region and is a fair approximation to the shape of the upper F region above the peak. The parameter g, which is a measure of the increase in scale height with height, does have a diurnal and geographic dependence and cannot be represented by a single constant. The obvious disadvantage to this model is the requirement for a true height ionogram analysis. Usually monthly median hourly ionograms are constructed and the true height analysis is done only once for each hour, making a total of 24 true height analyses required for each month.

3.2. THE AFCRL FIRST ORDER MID-LATITUDE TEC MODEL

A model of mid-latitude slab thickness was made at AFCRL [Klobuchar and Allen (1970)], which, when combined with either a predicted or an actual value of foF2, gives a time delay. This model is simply:

$$\text{TEC} = 1.24 \times 10^{13} (\text{foF2})^2 \left\{ 261 + 26 \sin \left[\frac{(h-9) \pi}{12} \right] + K \sin \left[\frac{(D-60) \pi}{183} \right] \right\}$$

where

H is the local hour at the subionospheric point where TEC is desired

K = 73 for local hours 06 to 19

K = 36 for 05 and 20 hours only

K = 0 for 21 to 04 hours

TEC is in el/M²

D is the day of the year

Since this model used only northern mid-latitude slab thickness values in its construction its use is limited to that geographic region.

3.3 SAMS0 STUDIES

The United States Air Force Space and Missile Systems Organization (SAMS0), interested in ionospheric errors in a proposed L-band satellite navigation system, funded three groups to construct and test models of the TEC over the Continental United States (CONUS), Puerto Rico, Hawaii, and Southern Alaska. These studies are now finished and results of two of the three groups have been published in final form. The main difference between the three studies consisted in the approaches to the modelling of the ionosphere that were taken. Stanford University [Waldman and daRosa, (1971)], one of the contractors, constructed a TEC model based only on TEC data. They essentially made a polynomial fit to TEC behavior as a function of solar activity and did a Fourier analysis of TEC diurnal behavior. This was done

for data from only two stations, one was Stanford, a mid-latitude station and the other, Hawaii, an equatorial anomaly station.

The second SAMSQ contractor, the University of Illinois [Rao, et al (1971)] used TEC data and predicted foF2 values for the ESSA prediction program to construct equivalent slab thickness values at one location, which was then assumed to be true over a second location. The ESSA foF2 prediction program then was used as a cornerstone of the data base along with the TEC data that were available to form predictions of TEC at another location.

The third contractor, the Applied Physics Laboratory of the Johns Hopkins University, made an ionospheric profile model based upon ESSA predicted foF2 values and theoretical values of profile shape above the height of the maximum of the F2 region. They used TEC experimental data only in the evaluation of the errors of their model but not in its construction.

3-4 NASA-DBA STUDIES

NASA, [Bent, et al (1971)], Goddard Space Flight Center, recently had completed for it a study of ionospheric profile modelling by the DBA Systems Incorporated Company of Melbourne, Florida. The NASA-DBA model is a profile model constructed using the ESSA foF2 prediction program for the peak density and the ESSA MUF predictions for the height of the ionosphere. Values of scale height above the peak were determined from analysis of topside ionosonde profiles.

3-5 COMMENTS ON MODEL STUDIES

All of the four F2 region models outlined have limitations due to the available data base. The most severely geographically limited model is perhaps the Stanford one, while the one which has the most world-wide applicability is perhaps the NASA-DBA model. Basically, there are at least two different philosophies presented by the four models just completed. One approach was to model TEC directly and only to use TEC data for this model. The opposite approach is to model the complete foF2 profile with the TEC being only a byproduct of the complete profile. These different approaches meet different needs. The TEC only model is of value where an adequate TEC data history exists to make a direct model and where only TEC is required. That is, this model is useful for error correcting from targets/satellites well above most of the ionization, say at least 1000 km in height. The profile model is necessary if the satellite/target is within the ionosphere and the integrated electron density only up to the height of the target is required.

3-6 THE PENNSYLVANIA STATE MARK I MODEL

A theoretical model of the ionosphere has been developed at the Pennsylvania State University [Nisbet (1971)] which attempts to describe the behavior of the ionosphere beginning with the basic processes which control the production, loss and transport of electrons. Experimental electron density values are used only to fit the boundary conditions. The model is basically for the mid-latitude ionosphere.

3-7 LIMITATIONS OF PRESENT MODEL STUDIES

The Stanford and Illinois results showed that the ionospheric time delay error can be reduced by 70-90 percent over the CONUS with the models they recently completed. Errors over Hawaii are substantially larger. No eastern longitude or Arctic latitude or southern hemispheric data were included in or tested against their models. The NASA-DBA profile model has not been checked against actual TEC data in a statistical way; however, the monthly median predictions of TEC from the NASA-DBA model fall within the extreme Stanford actual TEC monthly values for the periods that were tested in this manner.

All models suffer from incomplete data in the polar regions and the direct TEC model suffers because of the TEC data available which was limited to the United States.

3-8 ADVANTAGES OF COMBINED TEC AND SLAB THICKNESS MODEL

Using TEC obtained from polarization twist measurements from geostationary satellites and slab thickness values obtained from nearby ionosondings, continuous ionospheric measurements including a measure of the topside can be made. Topside satellite-borne sounders give only limited temporal coverage. The shape of the F2 region is not expected to vary as rapidly as the maximum density and hence the slab thickness parameter should be a good way to combine foF2 measurements or predictions with TEC measurements to make a TEC prediction at a distant point. It may also be reasonable to obtain a scale height from slab thickness values and make up a profile model using TEC measurements and the ESSA foF2 predictions. Providing the geostationary satellite with a suitable vhf transmitter is available for use, the TEC measurements are relatively easy to make.

References

- Bent, R. B. and Llewellyn, S. K. (1971) DBA Systems, Inc., and Schmid, P. E. (1971) NASA-GSFC, Greenbelt, Maryland, Ionospheric refraction corrections in satellite tracking, presented at the Open Meeting of Working Group I (a18) of the XIVth Meeting of COSPAR, Seattle, Washington.
- Klobuchar, J. A. and Allen, R. S. (1970) A First-Order Prediction Model of Total Electron Content Group Path Delay for a Midlatitude Ionosphere, AFCRL-70-0403.
- Nisbet, J. S. (1971) On the construction and use of a simple ionospheric model, Radio Science 6:437-464.
- Rao, N. N., Youakim, M. Y., and Yeh, K. C. (1971) Feasibility Study of Correcting for the Excess Time Delay of Transionospheric Navigational Ranging Signals, Technical Report No. 42, SAMSO TR71-163.
- Waldman, H. and daRosa, A. V. (1971) Prognostication of Ionospheric Electron Content, SAMSO TR-71-82, SEL-71-046.
- Wright, J. W. (1967) Ionospheric electron-density profiles with continuous gradients and underlying ionization corrections. III Practical procedures and some instructive examples, Radio Science, 2:10.

Contents	
4-1 Introduction	19
4-2 Stations Where TEC Data May Be Available	22
References	25

4. Available TEC and SLAB Thickness Data From S-66 Satellites

J.A. Klobuchar, J.P. Mullen and D.R. Seeman

4.1 INTRODUCTION

Many groups have made TEC measurements using the Faraday effect from VHF beacon signals on the S-66 (BE-B and BE-C) satellites. However, little effort has been made to use the available data from these stations to attempt to make a model of TEC, primarily because of the difficulty of combining data taken by several workers who used different data collection and reduction techniques, as well as different periods for compilation of seasonal average data. A few studies of short periods of data have been done. Frihagen [JSSG, (1968)] made a comparison of TEC obtained from a few satellite passes from several stations over Europe in January 1965. He showed that similar latitude gradients were obtained on several satellite passes taken from three different northern European stations. However, his limited data set precluded making meaningful synoptic maps of TEC. Houminer [JSSG, 1968B] made a comparison of TEC data from three low-altitude stations. The three stations had a similar diurnal TEC variation, with the equatorial station having higher TEC values but lower slab thickness values than the other two stations. His comparison was for only one season. Klobuchar and Aarons (1968) combined TEC data taken from Narssarsuaq, Greenland, Hamilton, Massachusetts, and Aricebo, Puerto Rico to obtain the TEC and slab thickness latitude dependence over the 5 to 65 deg North latitude range, but only for the March 1966 period. Galdon and Alberca (1971) studied the seasonal and solar cycle variation of mid-day TEC data taken during the 1965 through 1967 period from three European stations. They found similar

Preceding page blank

behavior with 10.7 cm solar flux for a 13 month running mean of TEC data from all three stations. After subtracting the 13 month running mean solar cycle dependence from the data, a large seasonal variation of TEC remained which changed with solar flux. The magnitude of the seasonal variation was different for all the three stations. They used only mid-day TEC data to determine the TEC solar flux dependence.

Several workers have constructed iso-contours of TEC versus latitude and local time for one or more seasons. TEC values over the range of plus and minus 10 to 15 deg of latitude can be obtained in this manner from a single station. These contours are helpful in determining the geographic regions and times where certain anomalies in TEC occur. All of the available TEC contours are included in the data section of this report.

Perhaps the best set of TEC contours was made by Amayenc, et al (1972) in which they combined the seasonal contours of Liszka (1967) with those from their own station at Val-Joyeux, near Paris, France to produce TEC contour maps versus local time over the European sector from 40 deg to 72 deg latitude for nine seasons in the 1964 to 1967 period. Since this geographic region is an important one for knowing the ionospheric time delay correction for a proposed VHF navigation system and for UHF satellite detection radars, it is fortunate that the work of Amayenc et al and Liszka has been done in this combined fashion. A separate section of this report details a numerical model of TEC, made from their data, for the year 1965, over the European longitude sector from 40 to 70 deg latitude. This model represents the most complete direct TEC data set available over Europe, though it is only for near sunspot minimum conditions. Several stations in Europe either have been, or currently are taking TEC data, using VHF beacons on a geostationary satellite, but, thus far, little of this data is in finished form for model studies.

While many papers in the literature give details of the behavior of TEC at a particular latitude, it is probably not possible to construct directly a complete model of TEC from the separate sets of published data. Fortunately, the slab thickness parameter S , does not change with latitude as much as either TEC or N_{\max} . Also, the variation of slab thickness with sunspot number is considerably smaller than that of either TEC or N_{\max} . Thus, the slab thickness parameter is worth investigating for model use. Since slab thickness values have been published for several stations having wide geographic distribution, these values have been scaled off the curves and the published data are given here. In a few cases these values of S were made from TEC data taken from observation of the Faraday effect on VHF signals from a geostationary satellite. A list of the stations for which S values are available is given in Table 4-1 along with the station's geographic coordinates, geomagnetic latitude and L value. Also, the season for which the data are available is indicated in the table. Figure 4-1 shows the behavior of S for the winter and summer seasons for the various stations for which data were available. Note that the daytime

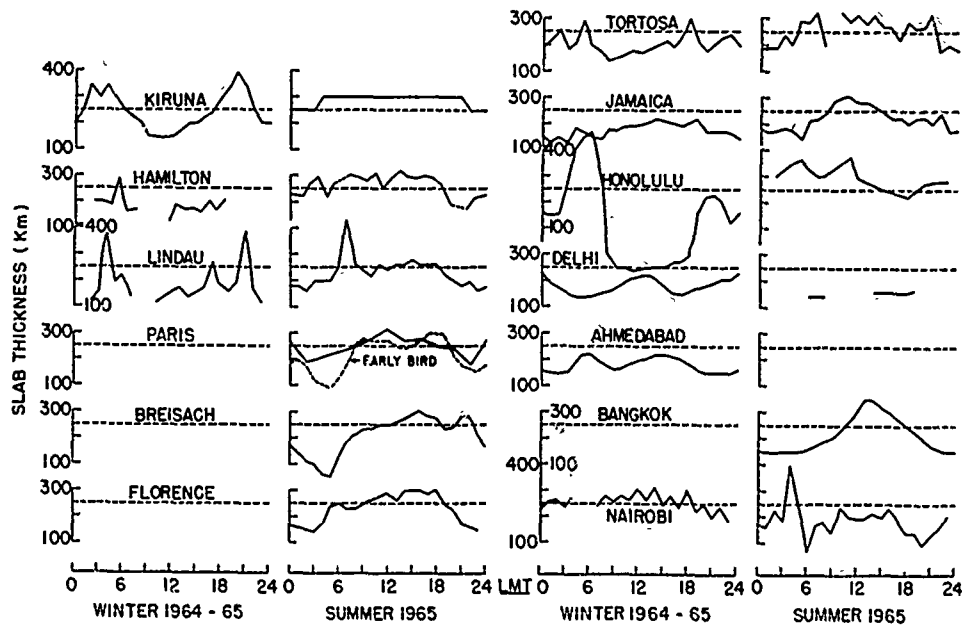


Figure 4-1. Equivalent Slab Thickness for Various Stations for Winter and Summer Seasons

Table 4-1. Stations Where Slab Thickness Values Have Been Published

	Geographic Latitude	Geographic Longitude	Geographic Latitude	L	* Season
Bangkok, Thailand	14.	100. E	2.4	0.91	3
Nairobi, Kenya	-1.33	36.8E	-4.4	1.01	1, 2, 3, 4
Ahmedabad, India	25.	72. E	13.8	1.00	1
Delhi, India	28.63	77.2E	18.9	1.08	1, 2, 3
Honolulu, Hawaii	20.0	200. E	21.1	1.14	1, 2, 3, 4
Haifa, Israel	32.9	283.2E	29.4	1.23	2
Kingston, Jamaica	18.0	35.1E	29.4	1.38	1, 2, 3, 4
Sydney, Australia	-33.8	150.6E	-42.3	1.87	1, 3
Tortosa, Spain	40.8	0.5E	43.9	1.57	1, 2, 3, 4
Florence, Italy	43.8	11.2E	44.7	1.70	3
Breisach, Germany	48.1	7.6E	49.5	2.08	3
Paris, France	48.8	2.0E	50.5	2.11	2, 3, 4
Lindau, Germany	51.	10. E	52.3	2.33	1, 2, 3, 4
Hamilton, Mass.	42.6	289.2E	54.1	3.11	
Kiruna, Sweden	67.8	20.4E	65.2	5.44	1, 2, 3, 4

* Key to seasons:

- 1 Winter, 1964-65
- 2 Spring, 1965
- 3 Summer, 1965
- 4 Autumn, 1965

(All seasons refer to the Northern Hemisphere)

values are much greater in summer at all latitudes, than in the winter. The large values of S found in the winter night at Honolulu, particularly near sunrise and sunset, may be due to small, systematic errors in TEC or to relatively large horizontal gradients between the TEC measurement sub-ionospheric point and the location of the ionosonde at those times.

Liszka (1967) has published iso-contours of equivalent vertical slab thickness for northern Europe for three seasons during the 1964 to 1965 time period. His iso-contours are given in the data section of this report. Also in the data section are examples of comparisons of slab thickness values taken at widely separated mid-latitude stations, indicating that the concept of modelling slab thickness, along with a knowledge of foF₂, to find TEC, is valid. As more TEC data become available, particularly from monitoring VHF radio waves from geostationary satellites, the behavior of slab thickness will become known better than at present.

4-2 STATIONS WHERE TEC DATA MAY BE AVAILABLE

An attempt has been made here to list the stations located throughout the world where TEC data may be available. These stations generally fall into several categories because of the availability of appropriate satellites. Generally those available fall into two distinct sets. The earliest set of data came from stations scattered throughout the world who obtained TEC from various low-altitude (approximately 1000 km) satellites. These satellites were the Transit series where a few stations obtained TEC from the differential Doppler effect, and, later, the S-66 satellites BE-B and BE-C, where most stations used the differential Faraday effect to obtain TEC. Beginning in the Pacific sector in 1964 some continuous TEC data have been obtained because of the availability of continuous VHF transmissions from a geostationary satellite. In 1965 the American sector first had the continuous availability of VHF signals from geostationary satellites. The European sector coverage has not been continuous due to the lack of VHF signals on geostationary satellites visible from Europe. Some European stations obtained continuous data during the summer of 1965, then sporadically beginning again in 1968. Thus, the available data are limited in various places, not only because of the obvious lack of stations in some areas but also due to the absence of a suitable satellite of opportunity having VHF transmissions from which the Faraday rotation measurement can be made. TEC values, when available from a station, are much more complete than those from low orbit satellites, as they are continuous. The low orbit data usually consists of a few points per day on a combined seasonal plot. Only in a few instances are latitude gradients available from the low orbit derived data.

Some errors are inevitable in any list such as this and the author apologizes in advance for any errors and omissions. They are unintentional. It is simply not possible to keep track of the work of all TEC experimenters and their data throughout the world at all times.

The stations have been grouped according to three world sectors: 1, the American sector; 2, the European-African sector; and 3, the Asian-Pacific sector. Also listed for each station are the approximate geographic coordinates for each station, the principal investigator or person otherwise responsible for the data, and, in cases where it is known, the availability of data signified by S if it consists of TEC values derived from a few passes per day of a low orbit satellite, and G if the data came from geostationary satellite beacon signals. The G data are, of course, continuous and presumed to be of better quality. These stations are listed in Table 4-2.

Table 4-2. Stations Where TEC Data May be Available

American Sector				
Station Name	Latitude	East Longitude	Principal Investigator and Affiliation	Data Available
Thule, Greenland	77	291	J. Klobuchar, AFCRL	G
College, Alaska	65	212	G. Stanley, U. of Alaska	S, G
Baker Lake, Canada	64	264	G. Swenson, U. of Illinois	S
Narsarsuaq, Greenland	61	315	A. Lundbak, Danish Meteorological Institute	G
Cold Bay, Alaska	55	197	K. C. Yeh, U. of Illinois	G
Goose Bay, Labrador	53	300	J. Klobuchar, AFCRL	G
Houghton, Michigan	47	271	G. Swenson, U. of Illinois	S
Hamilton, Massachusetts*	43	289	J. Klobuchar, AFCRL	S, W, G
London, Ontario	43	279	G. Lyon, U. of Western Ontario	S, G
Weston, Massachusetts	42	289	B. Reinisch, Lowell Tech. Research Foundation	S
University Park, Pennsylvania	41	282	W. Ross, Penn. State U.	S, W
Boulder, Colorado	40	255	K. Davies, National Oceanographic and Atmospheric Administration	
Ft. Monmouth, New Jersey	40	286	H. Solcher, Institute for Exploratory Research	S, G
Chesapeake Beach, Maryland	39	283	J. Goodman, Naval Research Labs	G
Blossom Point, Maryland	38	283	L. Blumle, NASA Goddard	S
Greenbelt, Maryland	38	283	S. Rangaswamy, NASA Goddard	G
Urbana, Illinois*	38	273	K. C. Yeh, University of Illinois	S, W, G
Stanford, California*	37	238	A. V. daRosa, Stanford University	S, G
Stanford, California	37	238	V. Eshleman, Stanford University Pioneer	
China Lake, California	35	243		W, G
Goldstone, California	35	243	B. Mulhall, Jet Propulsion Laboratory	G
Corona, California	34	243		W,
Los Angeles, California	34	242	S. Venkateswaran, U. of California at Los Angeles	G
College Station, Texas	31	264	J. German, Texas A & M	S
Arecibo, Puerto Rico	18	293	A. V. daRosa, Stanford University	G
Kingston, Jamaica	18	283	P. Chin, U. of the West Indies	G
Mahuatlan, Mexico	16	264		
Panama Canal Zone	9	280	J. Klobuchar, AFCRL	G
Lima, Peru	-11	283	A. V. daRosa, Stanford University	G

Table 4-2. (Continued)

Station Name	Latitude	East Longitude	Principal Investigator and Affiliation	Data Available
Huancayo, Peru	-12	285	A. Giesecke, Geophysical Institute of Peru	S, G
San Jose, Brazil	-23	315	F. de Mendonca	S, W, G (?)
Tucuman, Argentina	-27	297	S. Radicella, ?	S, W
Port Stanley	-51	303		S, W
European - African Sector				
Station Name	Latitude	East Longitude	Principal Investigator and Affiliation	Data Available
Tromso, Norway	70	19	O. Bratteng, Auroral Observatory	S, W
Kiruna, Sweden	68	21	L. Liszka, Kiruna Geophysical Observatory	S, W, G
Kjeiler, Norway	60	11	J. Frihagen, Norwegian Defense Research Establishment	S, W
Rude Skov, Denmark	56	12	A. Lundbak, Danish Meteorological Institute	S
Moscow, USSR	55	37	J. Al'pert, Izmiran	?
Kuhlungsborn	54	12		S, W
Lancaster, England	54	357	A. Hunter, U. of Lancaster	?
Jodrell Bank, England	53	358	G. N. Taylor, Royal Radar Establishment	S
Aberystwyth, Wales*	52	356	L. Kersey, U. of Wales	S, G
Lindau, Germany	52	10	G. Hartmann, Max-Planck Institute for Aeronomy	S, W, G
Bochum, Germany	51	7	H. Kaminski, Observatory of Bochum	S, W
Slough, England	51	359	E. Golton, Radio Research Station	
Lannion, France*	49	357	J. Papet-Lepine, National Center for the Study of Telecommunications	S, G
Breisach, Germany	48	8	C. Munther, Breisach Isospheric Institute	S, W
Florence, Italy	44	11	P. Checcacci, Institute for the Study of Electromagnetic Waves (IROE)	S, W, G
Val-Joyeux, France	44	4	F. Bertin, National Center for Scientific Studies (CNES)	S, W
Graz, Austria	41	15	R. Leitinger, U. of Graz	S, W, G
Tortosa, Spain	41	0	E. Galdon, Observatory of Ebro	S, W, G
Athens, Greece	38	23	D. Matsoukas, U. of Athens	S, W, G
Haifa, Israel	33	35	J. Mass., Haifa Radio Observatory	S, W, G
Addis Ababa, Ethiopia	9	38	P. Gouin, U. of Addis Ababa	S, W
Accra, Ghana	6	0	J. Koster, U. of Ghana	S, G
Nairobi, Kenya	-1	37	R. Kelleher, U. of Nairobi	S, G
Dar Es Salaam	-7	39	D. Osborne, U. of Dar Es Salaam	S, W
Asian - Pacific Sector				
Station Name	Latitude	East Longitude	Principal Investigator and Affiliation	Data Available
Tehran, Iran	36	51	K. Afshar, U. of Tehran	S
Tokyo, Japan	35	139	Y. Nakata, Radio Research Labs	S, G
New Delhi, India	28	77	A. P. Mitra, National Physical Lab	S, W
Taipei, Taiwan	25	121	K. Pai, National Taiwan U.	S, G
Ahmedabad, India	23	72	G. Rastogi, Physical Research Lab	S
Calcutta, India	23	89	S. Basu, U. of Calcutta	S
Hong Kong	22	114	G. Walker, U. of Hong Kong	S, G
Honolulu, Hawaii	21	202	P. Yuen, U. of Hawaii	S, G
Hyderabad, India	17	78	E. B. Rao, Defense Electronics Research Lab	S
Bangkok, Thailand	13	100	C. Rufenach, National Oceanographic and Atmospheric Administration	S, W
Singapore	1	104	E. Golton, Radio Research Station Slough, England	S
Brisbane, Queensland	-27	153	G. Bowman, U. of Queensland	S, W
Armidale, N. S. W. Australia	-30	152	F. Hibberd, U. of New England	S, G
Adelaide, South Australia	-35	138	B. Briggs, U. of Adelaide	?
Auckland, New Zealand*	-37	175	J. Titheridge, U. of Auckland	S, G
Sydney, Australia	-37	140	G. Munro, U. of Sydney	S
Melbourne, Australia	-38	145	E. Essex, LaTrobe University	S, G

Table 4-2. (Continued)

Station Name	Latitude	East Longitude	Principal Investigator and Affiliation	Data Available
Wellington, New Zealand	-41	174	J. Titheridge, U. of Auckland	S, G
Christchurch, New Zealand	-43	173	G. Stuart, Dept. of Scientific and Industrial Research	S, ?
Invercargill, New Zealand	-46	168	J. Titheridge, U. of Auckland	S, G
Campbell Island, New Zealand	-53	169	J. Mawdsley, Dominion Physical Laboratory, DSIR	S,

Key:

- S indicates data available from low-orbiting satellites
- G indicates data available from geostationary satellites
- W indicates data or information may be available from the World Data Center
- * indicates the principal investigator for this station may have limited data from other stations not listed.

References

- Amayenc, P., Bertin, P., and Papet-Lepine, J. (1971) Sur l'evolution latitudinale du contenu electronique, Annales de Geophysique, 27 (No. 3):345-357.
- Galdon, E., and Alberca, L.F. (1971) Seasonal and Solar Cycle Variation of Total Electron Content at Temperature latitudes, Scientific Report No. 4, Ebro Observatory, Totora, Spain.
- Joint Satellite Studies Group (1968) Planet Space Sci. 16:607-714.
- Joint Satellite Studies Group (1968) Planet Space Sci. 16:1289.
- Klobuchar, J. A. and Aarons, J. (1968) Electron content latitude dependence - March 1966 period, Annales de Geophysique 24(No. 3):885-888.
- Liszka, L. (1967) The high-latitude trough in ionospheric electron content, J. Atmos. Terr. Phys. 29:1243-1259.

Contents

5-1 Introduction	27
References	30

5. A Numerical Model of TEC Over Europe for Sunspot Minimum Conditions

J.A. Klobuchar

5-1. INTRODUCTION

Results of two studies of the TEC of the ionosphere over Europe have been given by Amayenc (1971). They presented contours of equal TEC values as a function of geographic latitude and local time over the 40 to 72 deg geographic latitude range over Europe for nine seasons in the 1964 to 1967 period. The TEC data shown in their iso-contour maps was taken from two stations in Europe, from Kiruna, Sweden, and from Val Joyeux, near Paris, France. Original glossy prints of the iso-contours in the Amayenc et al. paper were kindly provided by F. Bertin for use in this report. TEC hourly values were scaled from these glossy prints at 5 deg geographic latitude intervals and a Fourier time series expansion of harmonic number 4 was made to each latitude set. A least squares third degree polynomial then was fitted separately to each Fourier coefficient over the latitude range from 40 to 70 deg. The resultant coefficients equal 36 in number, one set of 4 polynomial coefficients to represent the latitude dependence of each of the 9 Fourier terms. Thus, a set of 36 numbers specify the seasonal mean TEC behavior over the 40 to 70 deg geographic latitude range. All that is necessary to obtain a value of TEC is to use the coefficients for the season desired, and to specify a latitude and local time. The model is in the following form:

$$TEC = DC + 2 \sum_{i=1}^4 C_i \cos(it - 2\pi\phi_i/24)$$

where

$$DC, C \text{ and } \phi = K_0 + \sum_{j=1}^3 K_j (\text{lat})^j \text{ for the appropriate } DC, C_i \text{ or } \phi_i \text{ term.}$$

The coefficient sets for the seasons are given in Table 5-1. Table 5-2 contains a list of the months in each season along with the mean observed 10.7 cm solar flux over each season. Note that the mean 10.7 cm solar flux was nearly the same for all 4 seasons.

In order to determine how well the numerical coefficients represent the actual data, the TEC values obtained from the model were subtracted from the original contour values at 5 deg latitude intervals. The resultant errors are shown for the four seasons in Figure 5-1. Differences less than 1×10^{16} were left blank as this is probably the experimental accuracy of the original data. Note that the model fit is good indeed, as evidenced by the large blank areas in the figure. Figure 5-2 is an iso-contour of TEC as constructed by the numerical model for season 1 of the four seasons. It compares well with the original iso-contour for this season which is shown in Figure 5-2.

This model should have use in determining average TEC values for a given season for time delays for satellite navigation and satellite detection radars operating in the VHF to UHF bands. It is not intended for use in a day to day operational mode, but as an average background model. It will be particularly useful as a representative TEC background model for the approaching 1974 to 1975 solar minimum conditions for system design studies for the European sector. Its use in polar or equatorial latitudes or at other than European longitudes is not recommended.

Table 5-1. Seasonal Coefficients Sets

SEASON	POLY. TERM	DC	C1	C2	C3	C4	FH11	FH12	FH13	FH14
1	CONSTANT	-.364E+02	.305E+02	-.871E+01	.591E+01	.867E+01	.337E+02	.717E+02	-.129E+04	-.152E+02
1	X	.254E+01	-.162E+01	.522E+00	-.345E+00	-.442E+00	-.123E+01	-.443E+01	.801E+02	.582E+00
1	X**2	-.498E-01	.299E-01	-.981E-02	.669E-02	.902E-02	.247E-01	.902E-01	-.150E+01	.180E-01
1	X**3	.306E-03	-.184E-03	.590E-04	-.423E-04	-.550E-04	-.129E-03	-.502E-03	.918E-02	-.383E-03
2	CONSTANT	-.239E+02	.200E+02	.103E+02	.368E+01	.652E+01	.457E+02	-.961E+01	.229E+03	.164E+03
2	X	.187E+01	-.105E+01	-.652E+00	-.198E+00	-.413E+00	-.183E+01	.725E+00	-.140E+02	-.803E+01
2	X**2	-.366E-01	.192E-01	.136E-01	.368E-02	.808E-02	.363E-01	-.362E-02	.286E+00	.135E+00
2	X**3	.225E-03	-.110E-03	-.508E-04	-.213E-04	-.519E-04	-.241E-03	-.222E-04	-.198E-02	-.753E-03
3	CONSTANT	.289E+02	.160E+02	-.281E+02	-.675E+01	-.257E+01	-.759E+02	.977E+02	-.429E+03	.402E+03
3	X	-.642E+00	-.660E+00	.167E+01	.458E+00	.209E+00	.956E+01	-.263E+01	.264E+02	-.262E+02
3	X**2	.101E-01	.950E-02	-.310E-01	-.925E-02	-.415E-02	-.183E+00	.580E-01	-.514E+00	.468E+00
3	X**3	-.519E-04	-.459E-04	.188E-03	.607E-04	.253E-04	.682E-03	-.485E-03	.324E-02	-.278E-02
4	CONSTANT	-.384E+02	.150E+02	-.167E-01	-.353E+01	-.489E+01	-.457E+02	-.576E+03	-.736E+03	.481E+03
4	X	.229E+01	-.750E+00	-.172E-01	.185E+00	.233E+00	.326E+01	.320E+02	.418E+02	-.224E+02
4	X**2	-.451E-01	.136E-01	.685E-03	-.304E-02	-.424E-02	-.728E-01	-.959E+00	-.788E+00	.418E+00
4	X**3	.280E-03	-.810E-04	-.555E-05	.162E-04	.263E-04	.444E-03	.313E-02	.472E-02	-.252E-02

Table 5-2. Seasonal Solar Flux

Season	Month	2800 MHz Observed Flux	Mean Seasonal Observed Flux
I	November, 1964	72.8	75.9
	December, 1964	77.5	
	January, 1965	77.5	
II	February, 1965	74.6	73.4
	March, 1965	73.8	
	April, 1965		
III	May, 1965	77.9	76.4
	June, 1965	77.0	
	July, 1965	74.3	
IV	August, 1965	74.8	76.9
	September, 1965	76.3	
	October, 1965	79.6	

Winter, 1964-1965

Latitude	Hour																							
	0	1	2	3	4	5	6	7	8	9	10	11	12	13	14	15	16	17	18	19	20	21	22	23
70											1						1							
65			1	1			-1	-1			1					-1	-1		1			-1	-1	-1
60			1	1			-1	-1								-1			1					
55	-1				1			-1	-1		1	1	1						1	1			-1	-1
50	-1			1																				-1
45																-1	-1						1	
40										1							-1	1	1					

Spring, 1965

Latitude	Hour																							
	0	1	2	3	4	5	6	7	8	9	10	11	12	13	14	15	16	17	18	19	20	21	22	23
70	1																							
65																	-1				-1	-1		-1
60																			1					
55															1			1						
50																					-1			
45																								
40																								

Summer, 1965

Latitude	Hour																							
	0	1	2	3	4	5	6	7	8	9	10	11	12	13	14	15	16	17	18	19	20	21	22	23
70																								
65				1			-1										-1							
60												-1												
55					-1	-1	-1													1	1	1	1	
50		-1	1	1	1						1		1							-2	-1		1	1
45	-1								-1	-1						-1		1			-1	-1	1	1
40	-1		1			-1		1										1		-1		1	1	-1

Autumn, 1965

Latitude	Hour																							
	0	1	2	3	4	5	6	7	8	9	10	11	12	13	14	15	16	17	18	19	20	21	22	23
70																								
65																								
60				1	1	1							-1	-1			1				1			
55	-1	-1		1	1	1						-1	-1	-1			1	1	1	1	1	1		-1
50												1		-1										-1
45																								
40																					1			

Figure 5-1. Difference Between Model and Actual TEC (Units of 10^{16} el/m²)

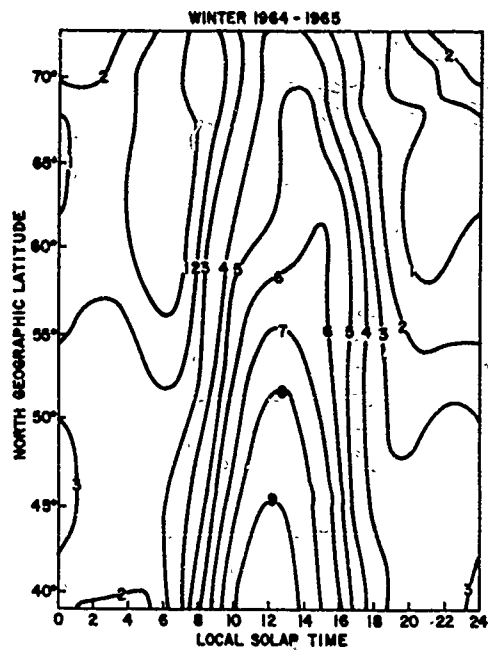


Figure 5-2a. Iso-Contour of TEC Northern Europe as Reconstructed by the Numerical Model, Winter 1964-65

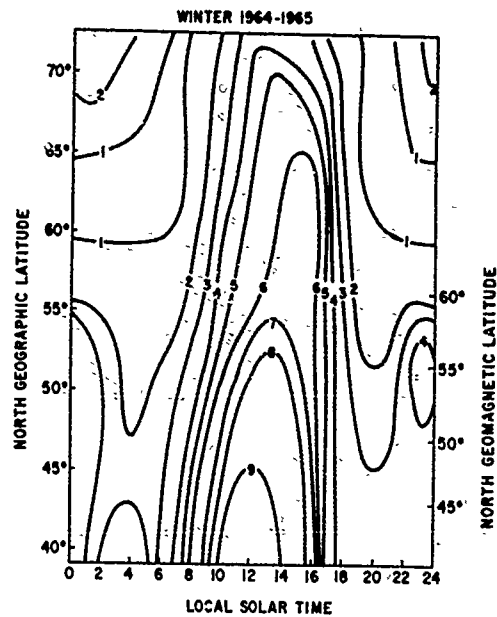


Figure 5-2b. Original Iso-Contour of TEC Over Northern Europe, Winter 1964-65

References

- Amayenc, P., Bertin, F. and Papet-Lepine, J. (1971) Sur l'evolution latitudinale du contenu electronique de l'ionosphere, *Annales de Geophysique* 27 (3):345-357.

6. A Comparison of TEC Obtained From Thomson Scatter and From Faraday Rotation

J.A. Klobuchar and S. Basu

6-1 A COMPARISON OF TEC COMBINED FROM THOMSON SCATTER AND FROM FARADAY ROTATION

Continuous measurements of TEC have been made for several years at Sagamore Hill, Hamilton, Massachusetts by observing the Faraday polarization twist of VHF radio waves transmitted from the geostationary satellite ATS-3. The ATS-3 satellite has been moved in longitude from time to time, but has spent much of its time nearly south of Hamilton, Mass. at an elevation of approximately 40 deg. The latitude below the point where the ray from Hamilton, Mass. to the satellite crosses the region of maximum electron density is approximately 39 deg North geographic.

Routine measurements of vertical ionospheric electron density profiles were made at Millstone Hill, Westford, Mass., 42.6 deg North, by J. V. Evans, Lincoln Laboratory, during a few days per month. In this section of the report comparisons are made between four days of vertical TEC taken by the Thomson scatter technique, kindly supplied by J. V. Evans, and "equivalent vertical TEC" obtained by looking at the Faraday polarization twist along the slant path to the ATS-3 satellite. The four days used in this comparison were magnetically quiet days, probably typical of the four different seasons during a sunspot maximum year.

The Thomson scatter data were usually available from a height below 200 km to 1200 km, though during some nighttime periods the signal-to-noise ratio was too poor to obtain data to 1200 km due to the low densities at very great heights. The TEC was obtained from the Thomson scatter data simply by integrating the profiles

throughout the height range for which data was provided. No extrapolation above 1200 km was made, nor was any attempt made to fill in data below the minimum height given by the Thomson scatter data. The profiles were integrated at approximate hourly intervals, during each of the four days.

The TEC derived from the Faraday effect was obtained by converting the observed Faraday polarization twist data to equivalent vertical TEC by using the longitudinal magnetic field and zenith angle at a fixed mean ionospheric height of 350 km. Results of model calculations have shown that the Faraday data obtain TEC out to heights of approximately 2000 km. Thus, the Faraday TEC should be greater than the Thomson scatter TEC, because it is integrated to approximately 2000 km, whereas the Thomson scatter TEC is integrated to a maximum of 1200 km. Also, there is an approximate 3 deg latitude difference between the locations of the two measurements, with the Faraday TEC being the farthest south. In this northern mid-latitude region gradients of electron density are usually lower at higher latitudes. These two factors should combine to make the Faraday TEC higher than the TEC obtained from the Thomson scatter.

Results of the four days of comparisons are shown in Figure 6-1. The agreement between the two sets of data on all four days is excellent. The largest difference between the two data sets occurs during the daytime afternoon periods when the latitude gradient of electron density between 42.6 deg North and 39 deg North is expected to be the largest. No attempt has been made to correct either data set for the effects of the expected latitude gradient. While the difference between the two data sets in the daytime period is likely due to the latitude gradient between the two observation latitudes, the observed difference at nighttime when the latitude gradient is small is probably due to the additional contribution to TEC above 1200 km in the Faraday data. This additional contribution also accounts for part of the daytime additional content observed in the Faraday data.

The one nighttime case when the Thomson scatter TEC was higher than the Faraday TEC occurred in the pre-dawn hours of January 17, 1969. The winter nighttime F region sometimes has relatively large gradients having small geographic extent. The pre-dawn dip observed in Faraday TEC, while a small nighttime increase was observed in Thomson scatter TEC was likely the result of such a winter nighttime gradient. Despite the small differences due to the reasons cited above, the TEC taken by the Faraday polarization twist method agrees well with the TEC obtained by integrating electron density profiles obtained by Thomson scatter.

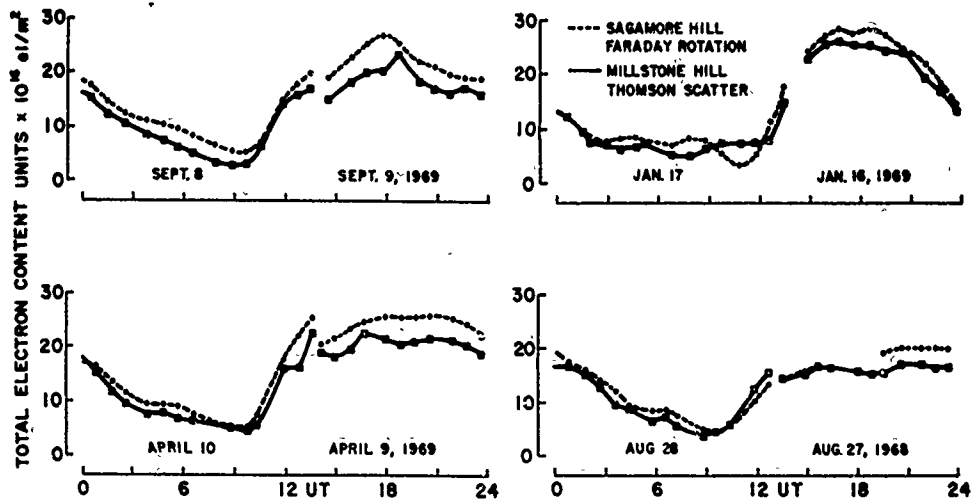


Figure 6-1. A Comparison of Total Electron Content Obtained From the Faraday Effect and From Thomson Scatter

Contents

7-1	Introduction	35
7-2	Equatorial TEC and Slab Thickness	35
7-3	Mid-Latitude TEC and Slab Thickness Data	37
7-4	The High Latitude Region	47
	References	53

7. Data From The Three World Ionospheric Regions

J.A. Klobuchar and D.R. Sosman

7-1 INTRODUCTION

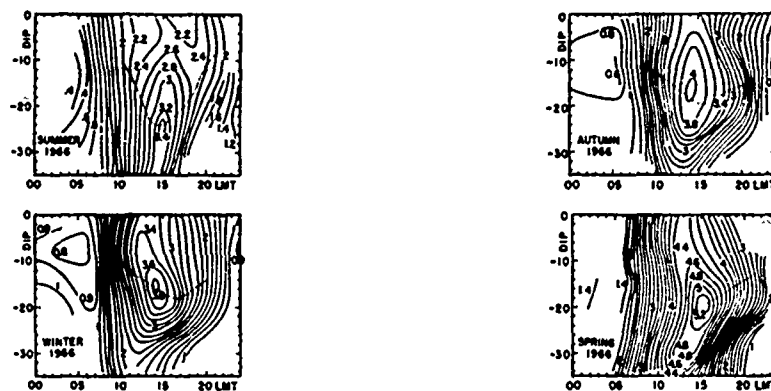
In this data section of the report, typical behavior of TEC, and, where available, slab thickness values are presented, along with a few comments on the general state of knowledge of TEC in each region.

7-2 EQUATORIAL TEC AND SLAB THICKNESS

The TEC of the equatorial region generally follows the same anomalous behavior as the density of the peak of the F region, N_{max} , that is, the TEC and N_{max} are not highest over the sub-solar latitude (the equator, for example, at the equinoxes). Both these parameters generally are highest at latitudes displaced on both sides of the dip equator.

One of the best summaries of TEC in the equatorial region was made by de Mendonca, et al (1969) by observing the Faraday effect from VHF signals transmitted from S-66 (BE-B and BE-C) satellites over Brazil in 1966. Their data was reduced in detail and plotted in the form of contour maps of constant TEC values over the dip latitude 0 deg to 35 deg South and 0-24 hours local mean time. Figure 7-1 shows de Mendonca's latitude-time contours of TEC for four seasons.

At Hawaii, which is located on the northern edge of the equatorial anomaly, a several year history of continuous TEC data has been compiled by monitoring Faraday polarization from VHF signals transmitted from one or more geostationary satellites. Yuen and Roelofs (1967) show much of this data.



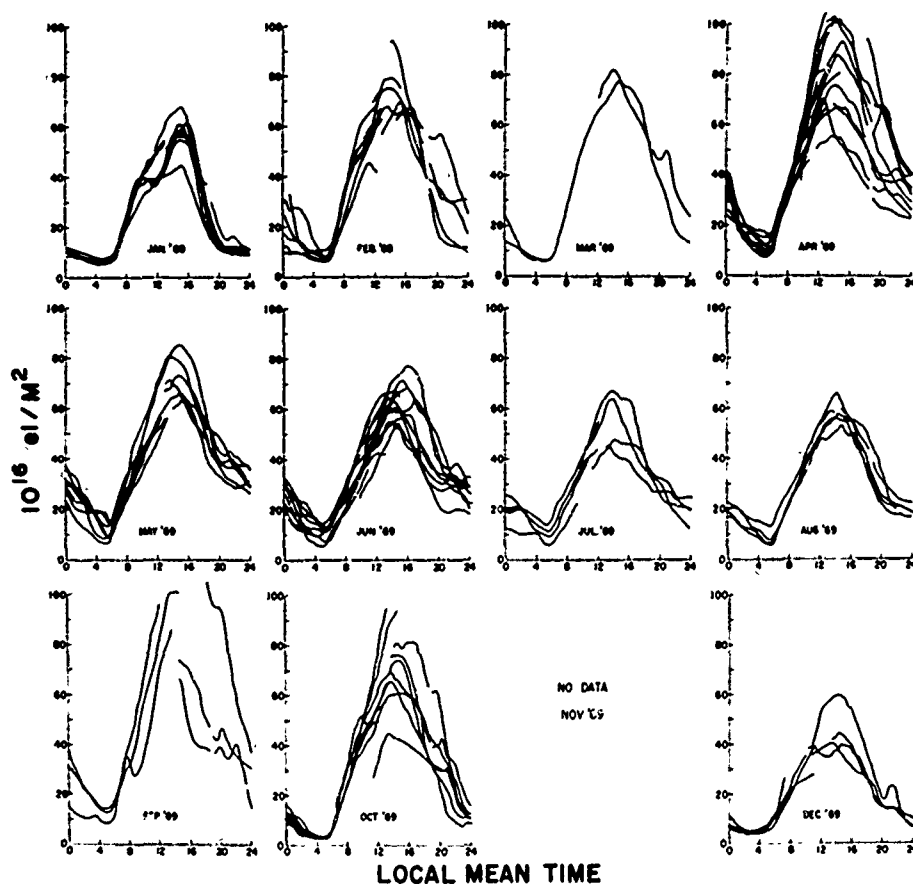


Figure 7-2. Total Electron Content for 1969 From the Panama Canal Zone

7-3 MID-LATITUDE TEC AND SLAB THICKNESS DATA

The TEC of the mid-latitude ionosphere is becoming fairly well known, at least over North America, where several stations have been making continuous TEC measurements for at least 5 years. A first order model of mid-latitude slab thickness has been discussed in this report as have several TEC models or complete vertical profile models from which TEC may be found. While these models may be available to system design engineers for correction for the effects of TEC on their system, these models say little or nothing about the statistical behavior of TEC, that is, its day to day variability. For this reason the following tabulated values of TEC are presented in this data section. Tables 7-1 through 7-6 give the mean, standard deviation, minimum and maximum values, median, upper and lower quartiles and upper and lower deciles of each hour of TEC and of equivalent slab

Table 7-1. Hourly Statistical Values of Total Electron Content and Equivalent Slab Thickness From Hamilton, Massachusetts, for January-February 1968

HOURLY VALUES OF TOTAL ELECTRON CONTENT VS. LMT																									
UNITS ARE IN ELECTRONS PER SQUARE METER COLUMN *10 ¹⁶ 16																									
JANUARY 1968																									
	1	2	3	4	5	6	7	8	9	10	11	12	13	14	15	16	17	18	19	20	21	22	23	24	25
MEAN	3.6	3.5	3.7	3.8	3.5	3.1	3.1	3.5	3.9	23.1	38.9	30.4	31.5	40.4	41.9	41.7	37.4	27.7	26.6	18.3	12.2	9.3	7.2	7.2	7.0
S.D.	1.4	2.0	2.0	2.0	2.3	2.0	1.7	1.4	1.4	3.3	6.6	4.3	2.4	5.3	6.0	1.1	6.1	6.5	7.2	4.5	3.7	7.6	3.3	2.9	
S MIN	1.0	1.3	1.3	2.0	2.3	2.1	2.1	1.5	12.2	17.0	27.8	25.2	21.0	21.4	30.0	35.1	28.1	44.7	15.2	17.0	7.1	5.2	4.7	7.5	
S MAX	12.1	11.2	15.0	15.1	14.7	11.2	14.6	5.8	10.2	10.0	41.7	45.9	44.2	50.2	50.4	57.4	56.1	53.7	41.1	15.0	28.4	22.4	15.3	17.4	
10.PCT	0.0	0.0	3.7	4.0	4.4	4.2	2.5	4.7	12.2	19.3	26.1	32.0	32.0	34.4	32.2	31.4	29.5	44.9	21.1	14.3	4.4	2.4	4.4	4.0	
25.PCT	1.2	1.2	4.4	5.2	4.9	4.1	4.2	3.4	13.1	20.2	27.1	33.0	33.2	36.7	37.0	37.2	30.7	19.4	21.1	15.5	4.1	7.0	1.5	4.7	
50.PCT	3.3	3.1	6.3	6.0	6.0	5.9	4.9	6.6	14.0	23.0	29.6	34.4	34.4	39.5	40.0	42.1	37.4	32.0	24.1	15.2	11.8	6.9	7.7	6.1	
75.PCT	7.7	7.5	7.5	7.7	7.3	6.8	5.9	7.4	16.2	25.0	34.0	39.4	41.5	42.8	45.4	43.8	41.0	26.3	28.9	19.0	13.9	10.1	7.2	7.7	
90.PCT	11.1	11.9	11.9	11.4	11.0	10.3	9.4	10.1	27.3	37.2	41.4	42.5	46.1	49.2	45.0	44.2	41.0	32.7	21.9	14.2	10.0	1.0	1.0	6.6	
COUNT	25	25	25	25	25	25	25	25	25	25	25	25	25	24	24	24	24	24	23	25	24	25	24	25	
HOURLY VALUES OF SLAB THICKNESS (M CP.) VS. LMT																									
JANUARY 1968																									
	1	2	3	4	5	6	7	8	9	10	11	12	13	14	15	16	17	18	19	20	21	22	23	24	25
MEAN	23.0	24.7	24.2	24.9	24.9	24.5	23.9	19.0	17.7	16.5	20.1	21.3	22.7	24.6	25.1	25.6	25.5	25.1	24.9	14.2	24.6	25.9	27.7	14.0	
S.D.	4.0	3.5	3.0	2.7	3.1	3.7	2.9	1.1	2.1	1.4	1.7	1.8	1.8	1.8	1.6	1.6	2.1	2.1	2.0	4.5	3.4	3.6	2.0	4.2	
S MIN	12.2	14.5	14.9	16.0	16.0	14.4	14.9	13.2	11.0	14.5	17.1	18.9	21.0	21.7	22.3	22.1	22.7	24.9	23.0	15.3	21.2	19.0	14.0	18.0	
S MAX	33.7	29.6	28.9	30.2	32.6	31.6	25.0	27.3	22.6	21.5	25.0	25.4	24.0	24.0	27.0	27.5	27.5	29.6	29.1	31.2	18.0	29.9	30.7	31.1	
10.PCT	21.3	23.9	23.9	24.4	24.4	24.4	24.4	24.4	16.1	16.1	19.1	21.0	22.0	22.0	22.0	23.0	23.0	23.0	23.0	14.2	24.6	22.0	19.0	21.0	
25.PCT	22.1	23.5	22.4	23.2	22.4	21.4	20.5	18.5	16.4	17.0	19.0	19.0	22.0	23.4	24.4	24.4	24.1	23.7	23.6	22.0	14.4	24.3	21.1	21.1	
50.PCT	24.6	24.7	25.7	25.0	24.0	23.0	19.0	17.9	18.5	20.1	21.3	22.2	24.1	25.7	27.1	25.6	24.7	24.7	24.7	13.6	24.9	25.7	25.9	26.8	
75.PCT	27.9	26.9	28.3	28.0	26.5	27.9	27.9	21.4	18.0	19.3	13.1	22.1	24.1	23.2	26.7	26.0	27.0	27.0	27.0	14.1	24.9	25.2	27.2	27.9	
90.PCT	31.2	28.2	27.1	27.4	26.0	24.1	22.4	21.1	19.5	21.0	23.1	24.2	26.9	27.0	27.0	28.0	27.0	27.0	27.0	13.7	27.5	27.9	29.7	21.3	
COUNT	24	25	24	25	24	25	24	25	23	25	25	25	24	24	24	24	24	24	24	24	24	24	24	25	
HOURLY VALUES OF TOTAL ELECTRON CONTENT VS. LMT																									
UNITS ARE IN ELECTRONS PER SQUARE METER COLUMN *10 ¹⁶ 16																									
FEBRUARY 1968																									
	1	2	3	4	5	6	7	8	9	10	11	12	13	14	15	16	17	18	19	20	21	22	23	24	25
MEAN	7.2	7.2	6.6	5.9	5.7	5.2	4.5	4.7	17.4	26.0	24.0	34.4	37.1	40.0	41.3	41.0	38.5	26.2	29.7	22.0	16.4	11.9	5.6	6.4	
S.D.	2.7	2.6	2.6	2.5	2.1	2.0	1.7	2.1	3.1	4.0	5.9	6.6	1.7	7.0	7.5	7.1	7.5	7.2	6.4	5.0	4.2	7.0	3.5	2.9	
S MIN	1.7	2.6	1.9	1.1	2.1	1.4	1.4	1.4	1.4	1.4	1.4	1.4	1.4	1.4	1.4	1.4	1.4	1.4	1.4	1.4	1.4	1.4	1.4	1.4	
S MAX	11.1	13.2	12.1	11.4	9.3	7.8	7.3	14.1	24.1	31.0	47.1	47.1	51.1	54.9	58.4	57.7	55.4	34.7	45.4	27.4	21.4	16.4	11.4	17.4	
10.PCT	0.4	1.7	3.3	2.0	3.1	2.1	1.9	6.5	12.9	18.3	27.0	26.0	31.1	37.7	32.3	33.4	39.1	37.7	23.4	15.3	10.1	6.3	5.2	4.9	
25.PCT	1.4	4.4	4.0	3.7	3.5	3.3	2.8	7.3	14.0	19.6	25.6	3.4	12.5	35.4	35.5	34.6	41.2	38.4	25.1	16.9	12.4	6.7	7.0	6.1	
50.PCT	7.4	7.0	6.8	6.4	6.3	5.9	4.6	8.1	16.0	21.3	28.5	32.7	31.5	37.4	38.0	34.1	37.2	34.0	25.1	16.4	10.1	6.0	7.0		
75.PCT	11.1	11.4	7.9	7.7	7.3	6.0	5.6	13.1	18.0	26.7	37.1	37.5	41.4	45.2	44.7	44.7	44.9	28.0	32.2	24.9	17.4	13.9	11.1	11.1	
90.PCT	11.1	11.7	9.2	8.1	7.7	7.3	6.0	11.9	22.4	29.6	37.4	44.9	46.1	51.0	47.2	50.6	47.0	44.0	33.5	25.9	21.7	16.7	17.0	18.0	
COUNT	25	25	25	25	25	24	25	25	25	25	25	25	25	25	21	21	21	24	24	24	23	24	24	24	
HOURLY VALUES OF SLAB THICKNESS (M CP.) VS. LMT																									
FEBRUARY 1968																									
	1	2	3	4	5	6	7	8	9	10	11	12	13	14	15	16	17	18	19	20	21	22	23	24	25
MEAN	25.2	24.5	23.7	23.9	23.0	24.7	24.4	21.6	19.4	20.1	12.0	22.4	24.1	25.9	25.0	21.7	20.1	16.1	26.5	27.9	23.2	25.0	21.7	19.0	
S.D.	5.7	4.6	5.0	5.3	5.1	6.1	4.2	4.2	2.0	2.0	2.4	2.1	2.3	4.2	3.0	1.5	3.7	4.7	4.9	3.1	2.0	4.2	3.4	4.2	
S MIN	11.0	9.5	8.1	8.1	6.3	5.0	3.5	1.5	1.3	1.3	1.3	1.3	1.3	1.3	1.3	1.3	1.3	1.3	1.3	1.3	1.3	1.3	1.3	1.3	
S MAX	43.6	43.5	38.3	32.3	31.0	37.0	37.0	32.0	24.7	27.4	20.1	20.1	25.0	42.0	33.0	32.0	39.2	33.1	32.7	24.0	34.0	23.1	14.9	17.0	
10.PCT	11.3	19.5	18.0	15.0	10.3	17.4	2.5	10.2	16.1	18.1	21.4	25.0	21.7	22.0	22.0	22.0	22.0	12.9	13.1	22.0	21.0	22.2	17.4	14.0	
25.PCT	21.3	27.3	21.2	19.5	21.9	22.1	21.7	19.0	18.9	18.5	4.1	11.0	22.0	23.4	23.7	24.1	24.4	14.5	24.1	14.4	21.0	23.4	23.0	22.9	
50.PCT	21.3	24.6	24.3	14.2	24.2	24.5	24.6	23.0	18.0	20.7	21.5	22.0	24.3	24.7	24.9	24.5	26.6	15.5	21.0	16.7	23.4	25.7	25.9	25.0	
75.PCT	27.3	27.1	26.1	15.0	24.4	27.5	24.6	21.0	21.1	22.1	22.6	24.1	24.4	26.4	27.6	27.6	27.6	20.2	20.2	27.0	21.0	20.0	17.0	27.0	
90.PCT	25.2	28.0	24.0	27.4	29.1	29.0	24.0	23.0	23.1	23.0	24.0	24.0	24.0	24.0	24.0	24.0	24.0	24.0	24.0	24.0	24.0	24.0	24.0	24.0	
COUNT	24	25	25	25	25	24	25	24	25	25	25	25	25	25	21	21	21	24	24	24	23	24	24	24	

Table 7-4. Hourly Statistical Values of Total Electron Content and Equivalent Slab Thickness From Hamilton, Massachusetts, for July-August 1968

HOURLY VALUES OF TOTAL ELECTRON CONTENT VS. LMT																								
UNITS ARE IN ELECTRONS PER SQUARE METER COLUMN *10 ¹⁶																								
JULY 1968																								
	1	2	3	4	5	6	7	8	9	10	11	12	13	14	15	16	17	18	19	20	21	22	23	
MEAN	11.3	8.6	7.5	6.7	6.1	6.6	5.8	17.5	16.1	15.2	16.2	16.7	17.6	17.7	18.4	19.3	20.1	20.1	20.5	20.7	16.2	15.7	12.5	11.7
StD.	1.8	1.7	1.5	1.5	1.3	1.1	1.5	1.8	2.2	2.6	2.6	2.6	2.5	2.9	3.6	3.6	3.9	3.8	3.6	3.8	2.7	2.1	1.7	1.8
S MIN	3.2	4.5	4.3	3.4	2.2	4.5	7.5	9.4	10.1	11.2	11.7	12.2	11.5	12.6	14.3	17.2	17.7	17.7	17.7	17.7	15.2	14.2	12.0	11.0
N MAX	13.6	11.4	11.4	9.1	7.4	9.9	14.7	17.6	20.1	19.7	22.5	21.0	22.6	24.9	31.2	37.9	37.7	29.0	29.0	29.0	24.6	23.1	18.0	16.3
10.PCT	7.4	5.0	5.0	3.8	3.2	6.7	8.5	13.3	10.7	11.8	13.6	13.7	12.4	14.3	16.8	19.7	16.3	16.3	16.1	15.6	14.1	12.8	11.1	8.9
25.PCT	7.1	7.0	6.6	5.3	4.1	5.7	8.8	11.9	12.5	14.3	13.7	14.0	15.1	15.6	16.4	17.4	18.1	18.8	18.4	18.4	16.2	14.3	11.7	10.7
50.PCT	11.5	8.9	7.6	6.2	5.3	6.9	5.4	12.1	14.0	15.2	15.9	16.5	16.4	17.0	17.7	18.7	19.1	19.0	19.0	17.7	15.9	14.1	11.9	11.0
75.PCT	11.6	9.4	8.5	7.4	6.2	7.6	16.2	13.2	15.0	17.2	18.1	19.3	15.2	19.0	19.6	21.1	20.7	21.0	21.2	21.9	19.1	16.8	14.3	11.1
90.PCT	11.6	11.4	5.1	7.0	6.0	7.8	11.5	13.9	16.4	16.1	19.5	20.0	21.4	21.7	22.1	22.4	23.2	23.5	24.1	24.0	21.8	18.6	15.6	13.6
COUNT	14	18	31	31	31	28	29	29	33	30	31	36	36	34	36	23	31	31	21	31	29	28	28	28
HOURLY VALUES OF SLAB THICKNESS (IN KM.) VS. LMT																								
JULY 1968																								
	1	2	3	4	5	6	7	8	9	10	11	12	13	14	15	16	17	18	19	20	21	22	23	
MEAN	249.	212.	229.	231.	232.	267.	258.	371.	293.	268.	291.	317.	328.	333.	363.	332.	336.	326.	319.	291.	290.	251.	277.	247.
StD.	31.	41.	37.	43.	49.	44.	25.	31.	45.	42.	47.	36.	21.	35.	31.	27.	26.	21.	27.	32.	29.	22.	14.	20.
S MIN	151.	179.	154.	146.	149.	249.	231.	237.	283.	212.	224.	229.	212.	241.	299.	271.	280.	251.	274.	234.	199.	217.	229.	176.
N MAX	311.	336.	331.	329.	350.	477.	372.	431.	397.	399.	372.	393.	356.	424.	442.	373.	442.	281.	372.	254.	296.	289.	318.	186.
10.PCT	136.	177.	149.	179.	170.	235.	244.	237.	231.	271.	141.	239.	249.	244.	302.	294.	287.	191.	272.	151.	210.	215.	232.	113.
25.PCT	210.	199.	209.	199.	201.	292.	257.	254.	262.	254.	295.	306.	307.	319.	315.	304.	281.	244.	244.	274.	226.	226.	236.	232.
50.PCT	261.	227.	226.	236.	230.	252.	285.	346.	290.	294.	327.	314.	329.	370.	371.	321.	231.	310.	280.	238.	253.	235.	251.	
75.PCT	274.	256.	239.	211.	244.	364.	319.	316.	321.	314.	315.	319.	349.	268.	354.	319.	352.	264.	370.	276.	278.	274.	243.	
90.PCT	278.	231.	272.	215.	264.	329.	350.	374.	349.	371.	375.	357.	368.	271.	313.	364.	252.	326.	214.	280.	277.	276.	289.	
COUNT	21	25	28	26	25	27	28	24	28	25	24	19	26	27	17	29	24	28	27	22	19	19	19	19
HOURLY VALUES OF TOTAL ELECTRON CONTENT VS. LMT																								
UNITS ARE IN ELECTRONS PER SQUARE METER COLUMN *10 ¹⁶																								
AUGUST 1968																								
	1	2	3	4	5	6	7	8	9	10	11	12	13	14	15	16	17	18	19	20	21	22	23	
MEAN	14.5	8.3	7.4	6.1	4.9	4.7	6.1	11.3	13.0	15.3	16.7	17.7	18.5	19.6	19.9	21.1	21.8	21.7	21.1	21.3	18.1	16.7	14.2	11.3
StD.	2.2	2.0	1.9	1.5	1.4	1.2	1.2	1.5	2.2	2.6	2.9	3.0	2.5	3.2	3.2	4.0	3.6	3.3	3.1	3.0	2.4	2.1	1.7	1.4
S MIN	3.0	4.9	4.2	2.7	1.8	2.4	3.4	3.5	9.6	10.9	11.6	12.1	12.2	14.3	13.6	14.7	14.0	15.1	16.3	11.8	9.6	8.7	7.6	
N MAX	15.3	14.9	14.1	8.9	7.4	9.5	14.2	14.1	17.2	20.8	21.9	23.7	26.5	29.5	24.3	24.6	27.2	27.7	27.1	26.4	24.4	21.3	18.5	17.3
10.PCT	3.5	1.8	5.3	4.0	3.1	3.1	4.5	7.1	10.5	11.0	13.7	13.0	13.4	14.7	15.4	17.9	18.1	18.0	17.2	17.2	15.4	11.4	11.1	8.3
25.PCT	7.6	6.7	5.8	4.9	3.5	3.8	7.1	11.1	12.5	13.2	14.3	15.6	16.1	16.1	17.5	17.4	18.2	20.1	21.1	21.4	18.4	16.3	12.7	10.7
50.PCT	11.1	8.7	7.4	6.5	4.9	4.7	6.3	11.5	13.6	14.7	16.4	17.9	19.2	20.4	20.4	21.1	20.1	21.7	21.9	22.1	18.1	14.5	11.0	10.5
75.PCT	11.1	11.1	8.3	6.9	5.8	5.8	6.9	12.1	15.0	16.0	19.4	21.1	21.7	22.1	21.9	23.2	23.7	24.6	24.6	23.0	18.1	13.2	12.3	
90.PCT	11.6	11.7	8.7	7.8	6.7	6.9	5.0	13.9	16.9	18.0	21.6	21.0	23.7	24.6	23.7	27.7	28.7	28.7	28.4	25.1	20.0	17.2	14.3	14.1
COUNT	29	29	29	29	23	24	24	24	25	29	24	19	29	29	29	24	31	31	28	28	25	28	28	28
HOURLY VALUES OF SLAB THICKNESS (IN KM.) VS. LMT																								
AUGUST 1968																								
	1	2	3	4	5	6	7	8	9	10	11	12	13	14	15	16	17	18	19	20	21	22	23	
MEAN	211.	236.	232.	229.	221.	249.	263.	259.	267.	275.	294.	317.	324.	321.	326.	327.	335.	334.	312.	288.	299.	272.	240.	270.
StD.	35.	44.	41.	36.	39.	41.	38.	38.	46.	47.	49.	38.	26.	34.	35.	36.	40.	34.	42.	44.	34.	34.	25.	27.
S MIN	179.	175.	137.	138.	161.	181.	155.	179.	166.	245.	216.	248.	276.	274.	276.	276.	283.	264.	262.	227.	212.	218.	174.	204.
N MAX	530.	393.	305.	210.	235.	314.	341.	327.	364.	364.	402.	388.	421.	395.	431.	437.	425.	412.	431.	389.	328.	319.	337.	144.
10.PCT	130.	179.	171.	160.	146.	211.	214.	219.	215.	245.	271.	241.	282.	281.	314.	287.	301.	272.	241.	221.	216.	149.	160.	
25.PCT	216.	214.	210.	190.	213.	224.	227.	236.	245.	263.	267.	245.	296.	297.	310.	287.	287.	287.	287.	246.	233.	213.	215.	
50.PCT	235.	226.	231.	222.	214.	241.	239.	246.	257.	270.	246.	310.	316.	314.	324.	323.	343.	314.	277.	277.	250.	240.	192.	
75.PCT	254.	247.	247.	244.	244.	264.	264.	264.	264.	264.	264.	264.	264.	264.	264.	264.	264.	264.	264.	264.	264.	264.	264.	264.
90.PCT	231.	250.	271.	254.	254.	257.	246.	318.	352.	374.	364.	313.	379.	350.	369.	393.	391.	371.	347.	281.	291.	279.	146.	
COUNT	22	23	21	13	2	24	25	26	22	27	28	27	27	27	28	24	24	24	29	25	27	23	14	14

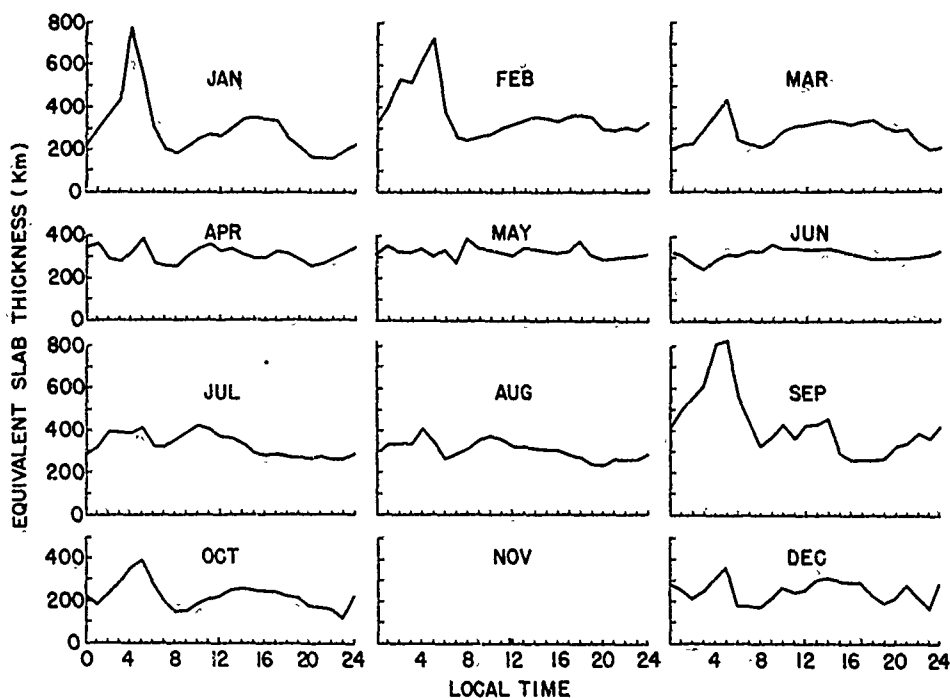


Figure 7-3. Monthly Median Equivalent Slab Thickness for 1969 From the Panama Canal Zone

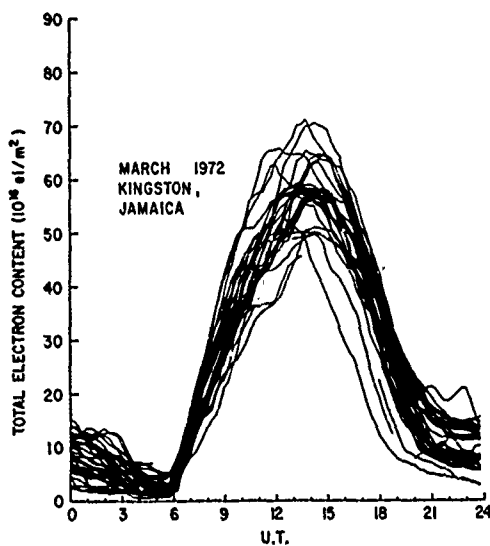


Figure 7-4. Total Electron Content From Kingston, Jamaica, West Indies, March 1972

thickness separately for each month of the year 1968 for data taken at Hamilton, Massachusetts. With these tabulated values, which are typical of mid-latitudes, a design engineer can determine, in addition to the average behavior, the complete statistical behavior of the mid-latitude TEC.

In order to show the relative good agreement between slab thickness values taken at widely separated mid-latitude stations, a series of graphs of slab thickness at pairs of stations is shown in Figures 7-5 through 7-8. All these stations are in the northern mid-latitude region. These curves show that a TEC model based upon slab thickness can

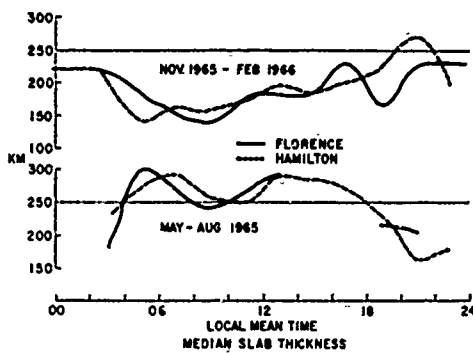


Figure 7-5. A Comparison of Seasonal Median Values of Slab Thickness at Florence, Italy, and Hamilton, Massachusetts

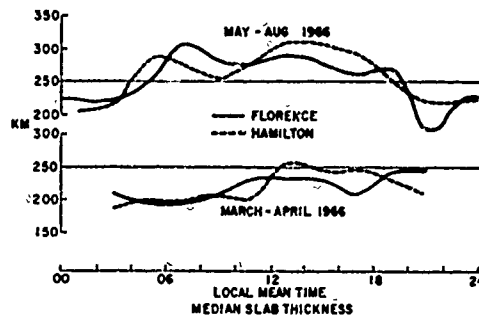


Figure 7-6. A Comparison of Seasonal Median Values of Slab Thickness at Florence, Italy, and Hamilton, Massachusetts

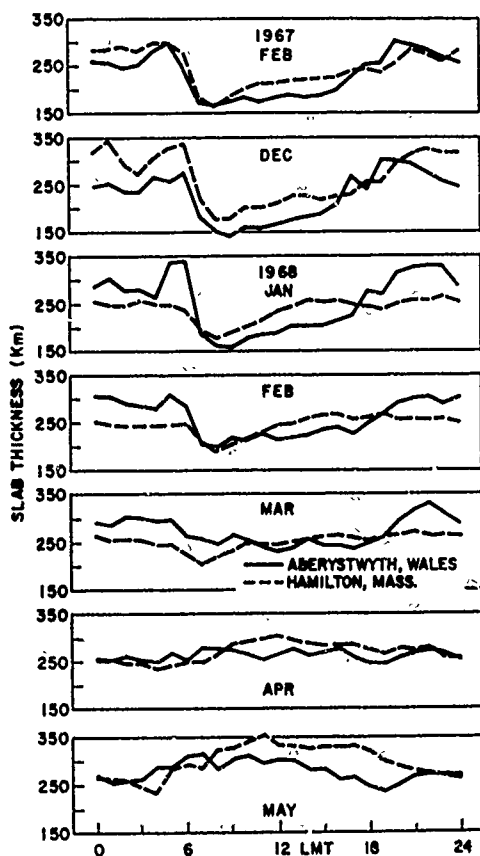


Figure 7-7a. A Comparison of Monthly Median Slab Thickness at Aberystwyth, Wales, and Hamilton, Massachusetts

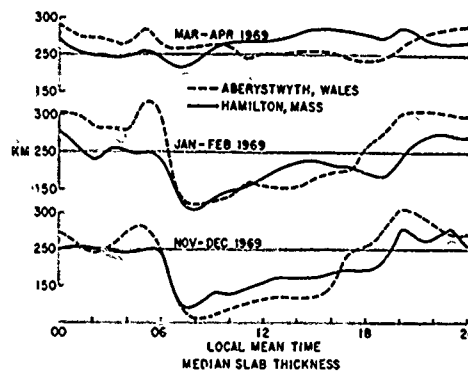


Figure 7-7b. A Comparison of Monthly Median Slab Thickness at Stanford, California, and Hamilton, Massachusetts

apply over this general region. The Stanford data was supplied through the courtesy of A. V. daRosa, the data from Aberystwyth, Wales by L. Kersley and the data from Florence, Italy is from P. F. Checcacci and M. T. deGiorgio (all private communications).

To give a picture of the average latitude and temporal behavior of the mid-latitude TEC for various seasons Figures 7-9 and 7-10 show TEC values taken from Hamilton, Massachusetts from the VHF signals from the S-66 (BE-B) satellite.

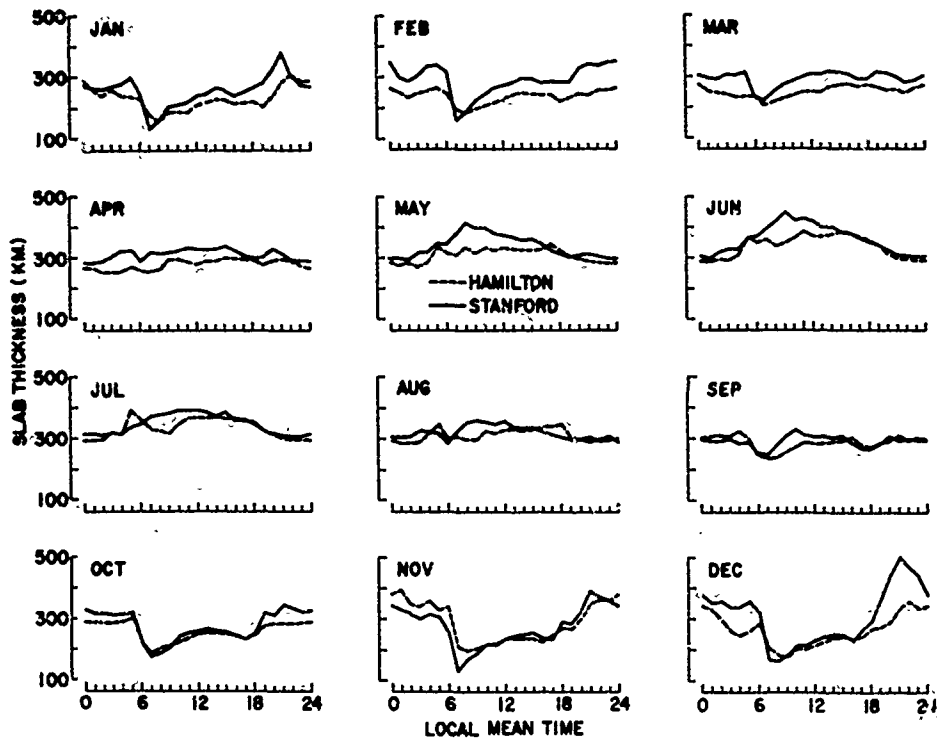


Figure 7-8. A Comparison of Monthly Median Slab Thickness at Stanford, California, and Hamilton, Massachusetts

Using the same satellite, observations of TEC have been made from Athens, Greece and are shown in Figure 7-11. These are kindly provided by D. Matsoukas (private communication). Figures 7-12 and 7-13 show the behavior of TEC over northern Europe for eight seasons. They are the result of combining data taken by Liszka (1967) with those taken at Val Joyeux, near Paris, France, Amayenc (1971). These contours were kindly supplied by F. Bertin for inclusion in this report. The first four of these contours were used to make the numerical model of TEC over Europe for sunspot minimum conditions, the details of which are in another section of this report.

While much work on TEC behavior has been done at a few other mid-latitude locations, such as in New Zealand, by Titheridge, and in Japan by Nakata, the stress on data presented here is on the Atlantic and European sectors because of NATO's particular interests in this region. The statistics given in Tables 7-1 through 7-6, along with the many TEC contours shown in Figures 7-9 through 7-13, depict fairly well the behavior of TEC in this region.

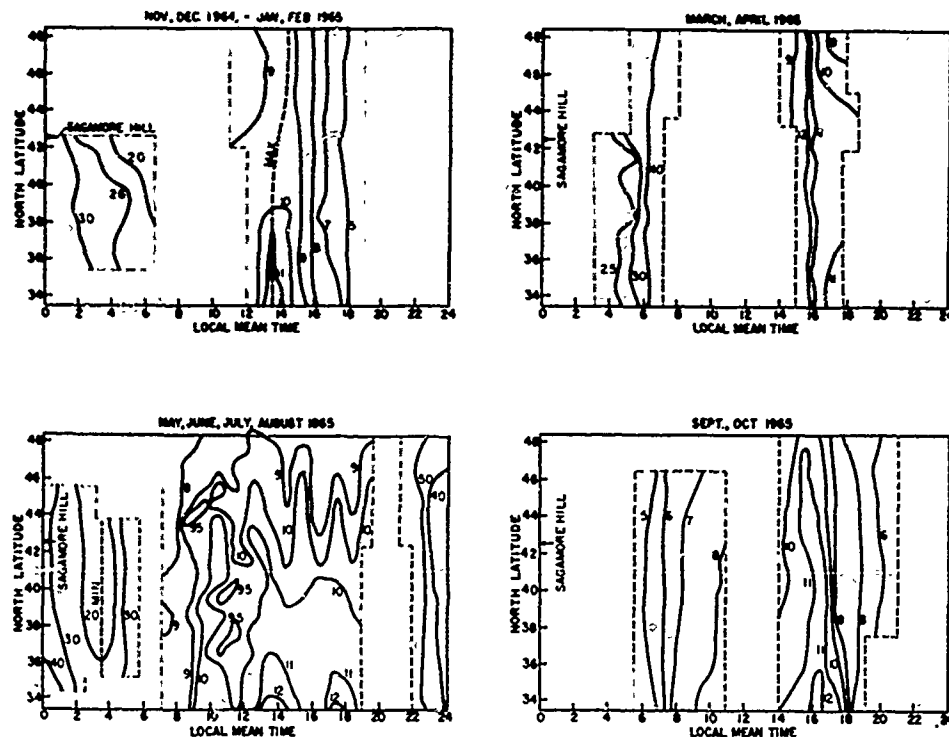


Figure 7-9: Iso-Contours of Seasonal Median Total Electron Content Taken at Sagamore Hill, Hamilton, Massachusetts

7.4. THE HIGH LATITUDE REGION

TEC measurements at the high latitudes have been made by only a few workers. Some of the important studies and their data are summarized here. TEC measurements using the S-66 (BE-B), 1000 km height, satellite were made from Kiruna, Sweden (67 deg-North, 20 deg East) geographic coordinates by Liszka (1967). A trough in the latitude distribution of TEC was sometimes observed on individual passes, particularly during the winter nighttime when it was always observed. Because the satellite is generally viewed at an oblique angle, sharp gradients in TEC are smoothed by this measuring technique. Liszka constructed iso-contour maps of TEC versus latitude and local-time for all hours for 9 three-month seasons over the latitude range from 55 to 72 deg North over the European sector. These contours are shown in the mid-latitude portion of the data section as they were attached to the mid-latitude TEC contours taken near Paris by Amayenc, et al. The trough in TEC is clearly seen in both the winter nighttime contours of the winter

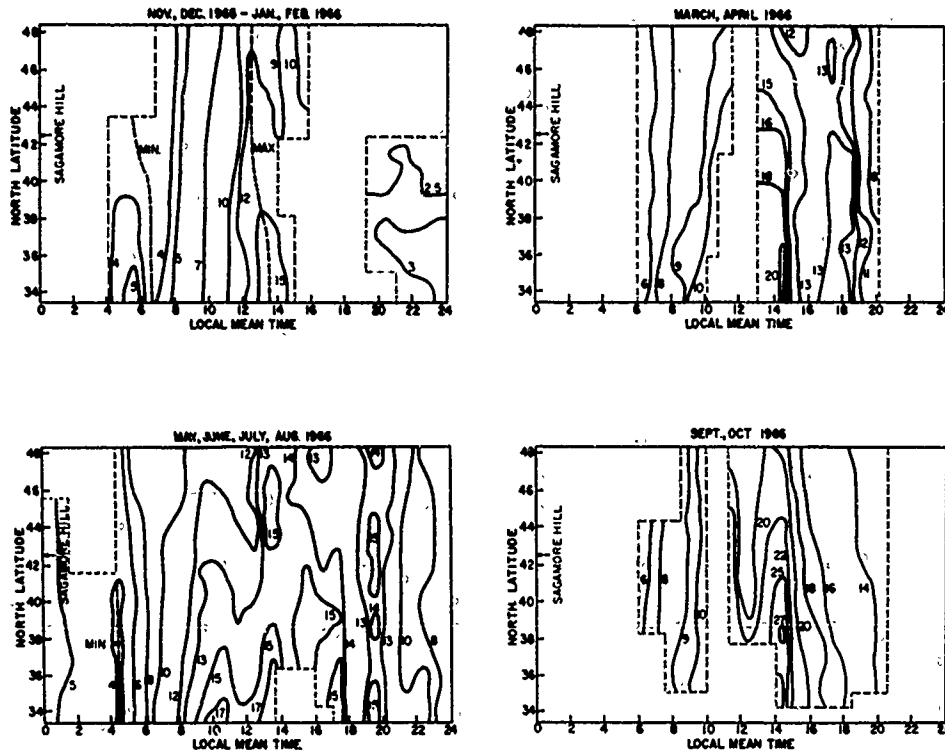


Figure 7-10. Iso-Contours of Seasonal Median Total Electron Content Taken at Sagamore Hill, Hamilton, Massachusetts

1964 to 1965 and the winter of 1965 to 1966. Though there is some evidence of the trough during the equinox periods, the rapid seasonal changes which occur at these high geographical latitudes were responsible for averaging both day and night values into the equinox contours, thus smoothing out any nighttime trough. Contours of the equivalent slab thickness parameter, over a 10 deg latitude range, were constructed by Litzka for four seasons by combining his TEC observations with foF2 observations from six Scandinavian ionosondes. These results are shown in Figure 7-14. In the winter two distinct maxima in slab thickness are clearly visible, one at 21 hours and the second at 03 hours local time. Both occur at 65 deg North geographic latitude. These maxima occur when the trough is above the Kiruna station.

Bratteng and Frihagen (1969) reported the results of TEC measurements made at Spitzbergen (78 deg North, 14 deg East). They constructed iso-contours of TEC versus local time for the Spring and Autumn 1965 periods. Their contours are reproduced in Figure 7-15. They noted the large 0900 LMT maximum in TEC at 78 deg North, but little evidence of a trough during the seasons shown is noticeable. Mikkelsen (1971) combined observations of TEC taken at St. John's, Newfoundland

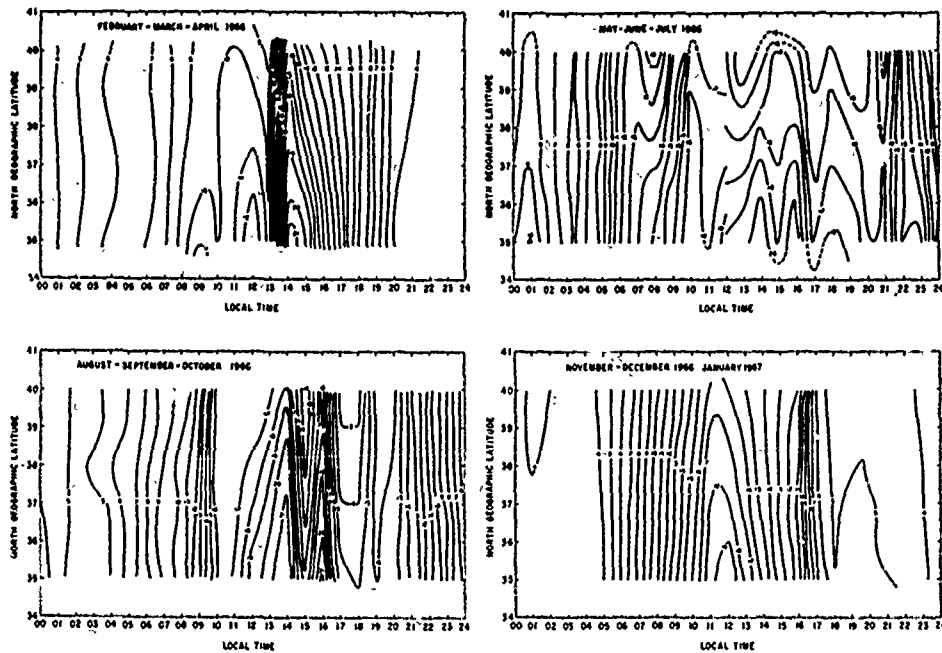


Figure 7-11. Iso-Contours of Seasonal Median Total Electron Content Taken at Athens, Greece

and Narssarssuaq, Greenland during July 1969 using the S-66 beacon satellite transmissions. He found a knee in TEC which moved southward with increasing magnetic activity, but not very good agreement between the position of the knee and that of the southern edge of the scintillation boundary. No mean data was shown by Mikkelsen either for TEC versus latitude or time.

Rai and Hook (1967) made TEC observations near College, Alaska during the winter of 1963-1964. They found a large secondary nighttime maximum in TEC near local midnight between 65 deg and 75 deg North geographic latitude. At 60 deg North there was only a slight nighttime increase. During magnetically disturbed conditions, they found large positive gradients towards the North. They reported no measurements of slab thickness.

Currently, continuous measurements of TEC are being taken at several high-latitude locations using the VHF signals transmitted from the geostationary satellite ATS-3. Stations where reduced data will soon be available include Narssarssuaq, Greenland, Goose Bay, Labrador, and College, Alaska. Some three months of data from Thule, Greenland have been reduced and are outlined in the following section.

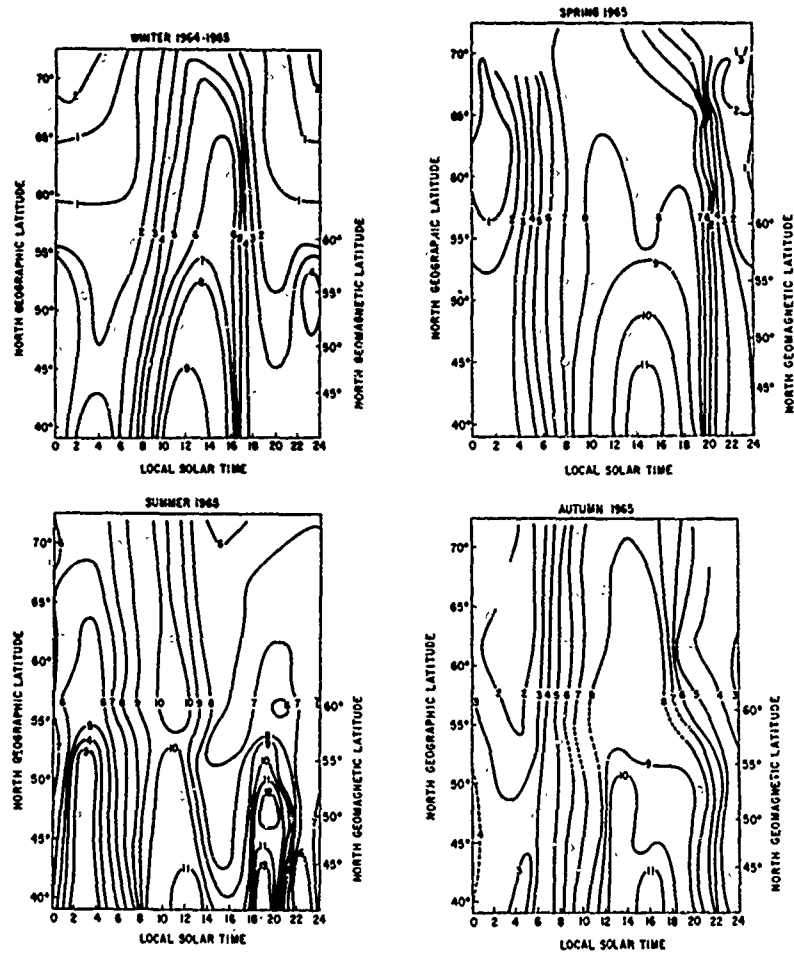


Figure 7-12. Iso-Contours of Seasonal Median Total Electron Content Taken Over Northern Europe in 1965 (After Amayenc et al, Annales de Geophysique, 1971)

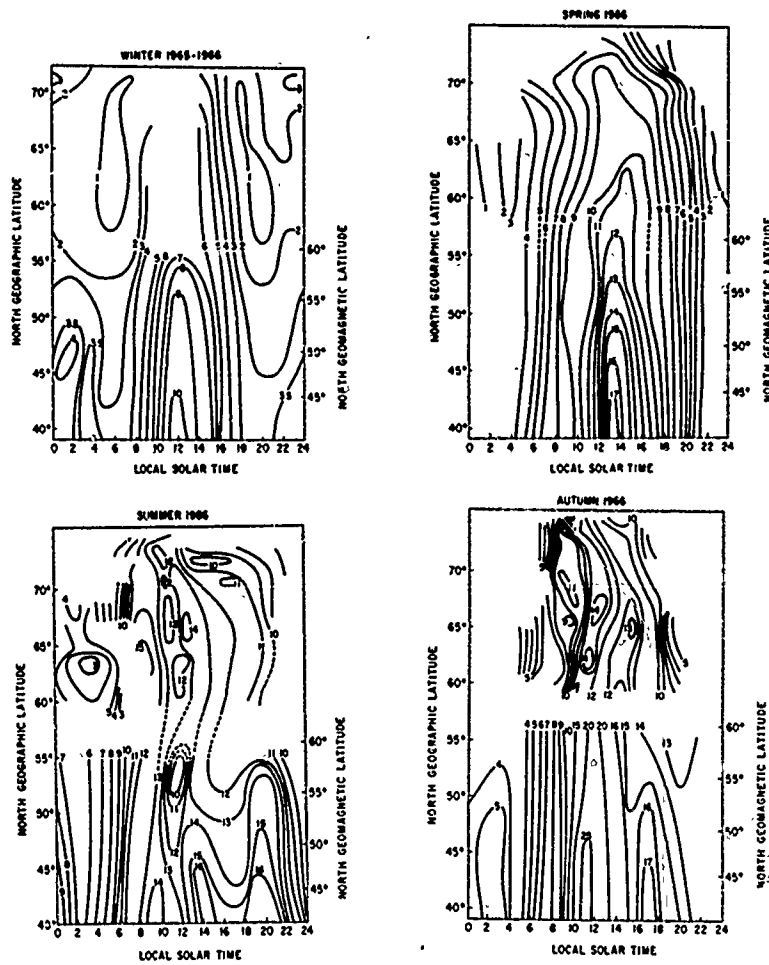


Figure 7-13. Iso-Contours of Seasonal Median Total Electron Content Taken Over Northern Europe in 1966 (After Amayenc et al, Annales de Geophysique, 1971)

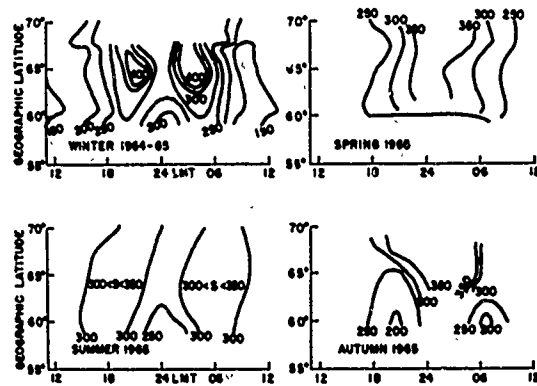


Figure 7-14. Contours of Equivalent Slab Thickness Over Northern Europe - 1965 (after Liszka, 1967)

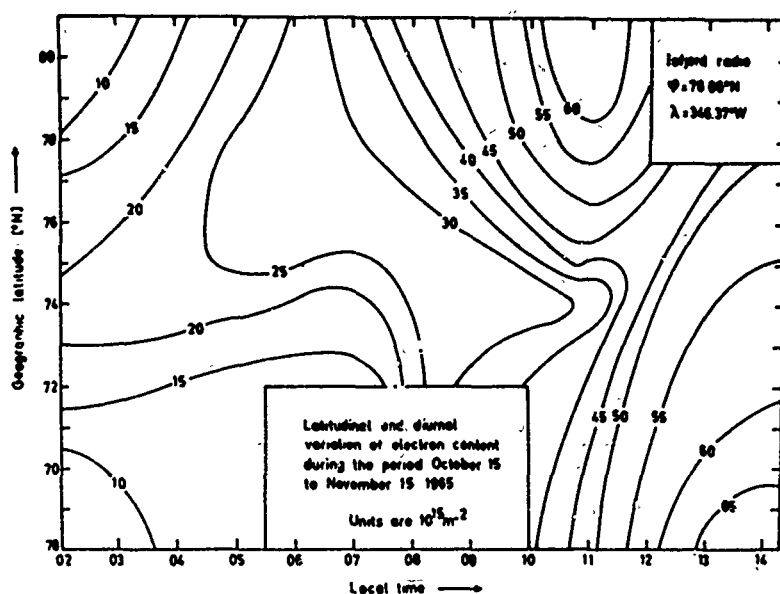


Figure 7-15a. Contour Map of Electron Content in a Geographic Latitude-LMT Plane for the Period 15/3-15/4/66 (After Bratteng and Frihagen, 1969)

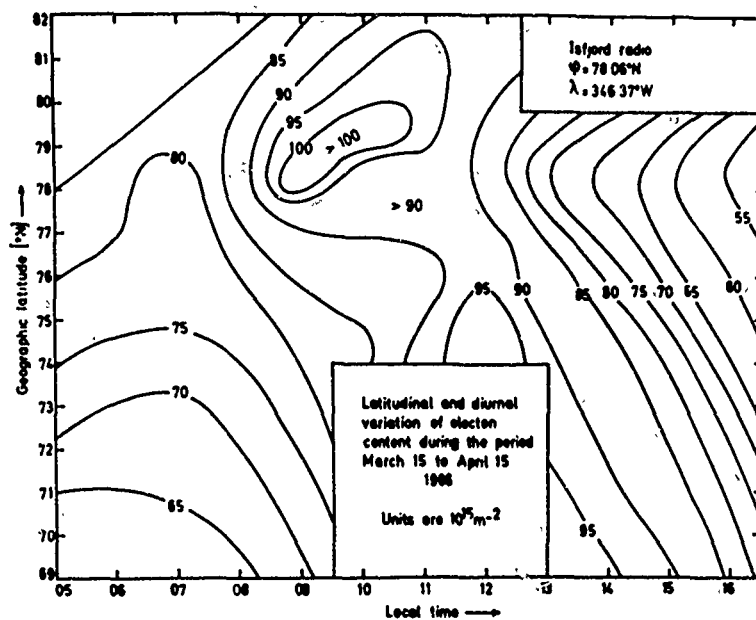


Figure 7-15b. Contour Map of Electron Content in a Geographic Latitude-LMT Plane for the Period 15/10-15/11/65 (After Bratteng and Frihagen, 1969)

References

- Basu, S. and Das Gupta, A. (1967) Latitude variation of total electron content in the equatorial region, J. Geophys. Res., 72:5555-5558.
- Blumle, L. J. (1962) Satellite observations of the equatorial ionosphere, J. Geophys. Res., 67:4601-4605.
- Bratteng, O. M. and Frihagen, J. (1969) The electron content in the polar F-region, The Auroral Observatory, Tromso, Norway
- de Mendonca, Kantor, I. J. and Iemsha, B. Low Latitude Ionospheric Electron Content Measurements During Half a Solar Cycle, Scientific Report LAFE-84, Laboratory of Space Physics, Sao Paulo, Brazil.
- Hunter, A. N., Webster, Kelleher, R. F. and Maill, P. E. (1965) Diurnal variation of total electron content of the ionosphere over Nairobi, Nature, 206:920-921.
- Liszka, L. (1967) The high latitude trough in ionospheric electron content, J. Atmos. Terr. Phys., 29:1243-1259.
- Mikkelsen, I. B. (1971) Knee of total electron content and scintillation boundary, Danish Meteorological Institute, Geophysical Papers R-21.
- Rai, S. B., and Hook, J. L. (1967) Total electron content and its variations in the auroral zone ionosphere during winter, J. Geophys. Res., 72:5319-5324.
- Rufenach, C. L., Nimit, V. and Leo, R. E. (1968) Faraday rotation measurements of electron content near the magnetic equator, J. Geophys. Res. 73:2459-2468.
- Yuen, P. C., and Roelofs, T. H. (1967) Seasonal variations in ionospheric total electron content, J. Atmos. Terr. Phys. 29:321-326.

Contents		
8-1	Introduction	55
8-2	Description of the Data	56
8-3	The Influence of Geomagnetic Disturbances	57
8-4	Discussion	59
	References	60

8. Low Elevation Angle Measurements of Total Electron Content Taken From Thule, Greenland

M. Mendillo and J.A. Klobuchar

8-1 INTRODUCTION

Continuous measurements of the Faraday polarization twist of VHF radio waves from the geostationary satellite ATS-3 have been made from April 1971, at Thule, Greenland (75.5 deg North, 68.7 deg West). This set of data represents the first attempt made from such a high latitude site to continuously monitor the diurnal behavior of the ionospheric total electron content (TEC). During this period the ATS-3 satellite was close to the Thule meridian (70 deg West) at a ground elevation angle of approximately 5 deg. Figure 8-1 shows the sub-ionospheric geographic latitude versus ionospheric height together with the L value at the Faraday rotation factor $\bar{M}(E\cos\theta\sec\chi)$ along the ray path to ATS-3. Note that the ionospheric station at Narssarssuaq, Greenland (61.2 deg North 45.4 deg West), is located at the same geographic latitude as the 400 km sub-ionospheric coordinates. The L shell at this point is 11.6 which corresponds to an invariant latitude (Λ) of 73 deg.

The values of polarization twist (Q) recorded at Thule have been converted to "equivalent vertical" electron contents (N_T) using $Q = \frac{K}{f^2} MN_T$ with the mean \bar{M} factor computed for an ionospheric height of 400 km. It should be noted that over the height range 300 to 500 km M changes by only 7 percent, and thus the decision at which height M should be chosen has more of an effect on determining the sub-ionospheric coordinates than it does on the derived values of N_T . The polarimeter in use at Thule has been calibrated only tentatively for absolute polarization reference, and therefore the absolute scale for the TEC curves was arbitrarily chosen to give

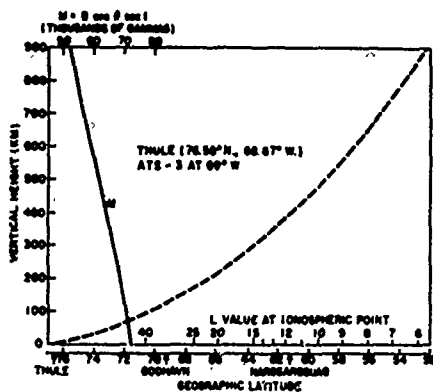


Figure 8-1. Sub-Ionospheric Latitude and M Factor vs Vertical Height From Thule Viewing ATS-3 Along the Station Meridian

reasonable values of slab thickness ($\tau = N_T / N_{max}$). It should be emphasized, however, that the data are continuous over an approximate three month period and thus day-to-day and seasonal differences may confidently be compared on a relative basis.

Before presenting our preliminary results, we would like to comment briefly on the appropriateness of constructing "equivalent vertical" TEC values using the Faraday rotation technique with a satellite only 5 deg off the horizon.

Model calculations were performed for day and nighttime equinox conditions using the geometry depicted in Figure 8-1.

The electron density versus height and latitude were taken from Chan and Colin (1969) for the topside with extrapolated values for the bottomside. When the amounts of rotation computed along the slant path through the ionosphere were converted to equivalent vertical N_T values using M at 400 km, the daytime results agreed to within 3 percent and the nighttime to within 7 percent of the actual vertical integrated profiles passing through the 400 km sub-ionospheric point. Several of the factors which contribute to this good agreement are:

- (1) Since \bar{M} and N_e decrease both with height and to the south, most of the rotation occurs where the ray path intersects the F2 peak.
- (2) The latitudinal N_e gradients southwards towards the trough are not too great at ionospheric heights near h_{max} .
- (3) While the elevation angle to ATS-3 is only 5 deg at the ground ($\sec \chi = 11.7$), at 400 km along the ray path it is 20 deg ($\sec \chi = 3.0$).

8-2 DESCRIPTION OF THE DATA

In Figure 8-2 data from the first three months of operation are given in a mass-plot format. The tendency for the TEC to have preferred values occurs because the received polarization is a combination of a direct ray from the satellite and a ground reflected ray of constant horizontal polarization. The contamination from the ground reflected ray is due to the low elevation angle at which these observations were made using modest gain yagi antennas. Despite this problem, some of the features clearly

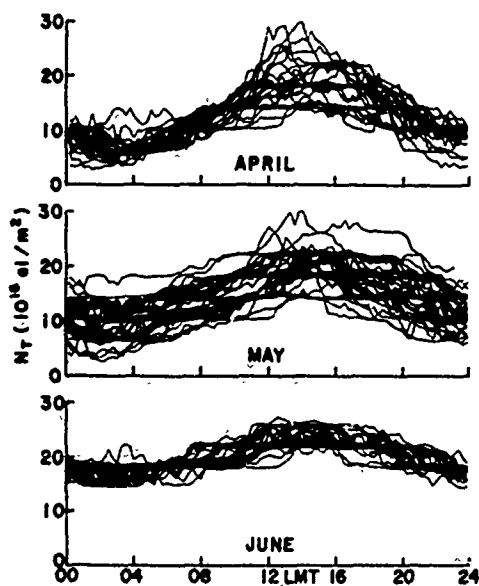


Figure 8-2. Total Electron Content From ATS-3, Thule, Greenland, 1971. Monthly overplots of all data

8×10^{16} el/m², respectively. Finally, the small arrows in Figure 8-3 give the times of ground sunrise and sunset at 61 deg North. It appears that as the daylength increases with season, the slopes (dN_T/dt) at sunrise and sunset both decrease.

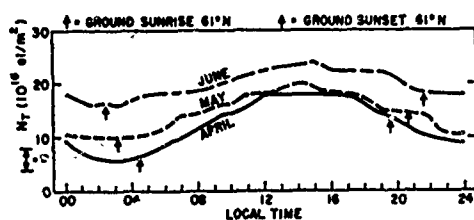


Figure 8-3. Total Electron Content From ATS-3, Thule, Greenland, 1971. Monthly medians

that both of the "ionospheric storms" took the form of an initial positive phase followed by a longer negative phase. This type of storm-time (Dst) behavior is quite similar to that normally found at mid-latitudes [Hibberd and Ross, (1967); and Mendillo (1971)]. With only two storm periods available, however, it is not

visible in Figure 8-2 include a diurnal effect with a broad afternoon maximum, a day-to-day variability, and also a great deal of structure at virtually all local times. The monthly median curves (\bar{N}_T) are presented in Figure 8-3. One can see that a seasonal trend is apparent in that at all local times \bar{N}_T (June) $>$ \bar{N}_T (May) $>$ \bar{N}_T (April) with the nighttime values showing the greatest change. At mid-latitudes, on the other hand, the seasonal variation during the daytime hours is quite different, that is, daytime \bar{N}_T values in June are significantly lower than the corresponding \bar{N}_T values in April. Figure 8-3 also shows that the overall diurnal range, that is, $\bar{N}_T(\max) - \bar{N}_T(\min)$, also varies with season. During April, the range is 12×10^{16} el/m² while during May and June it reduces to 10 and

8-3. THE INFLUENCE OF GEOMAGNETIC DISTURBANCES

In order to investigate the effects of magnetic activity, we concentrated on the April 9 to 30 period. During this time, two moderately severe sudden commencement storms occurred and in both cases there were recognizable departures in N_T from monthly median conditions.

From Figures 8-4a and b one can see

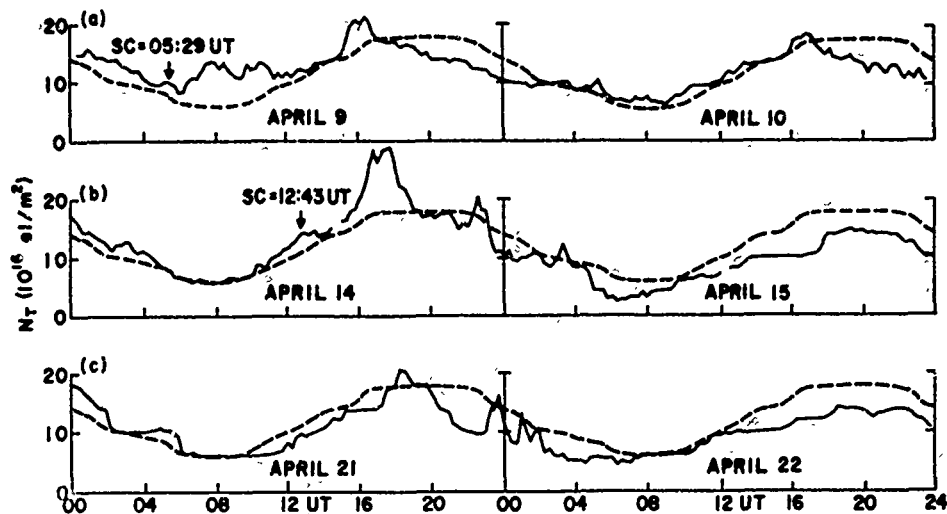


Figure 8-4. Total Electron Content from ATS-3, Thule, Greenland, During One Quiet and Two Disturbed Periods in April 1971

possible to discuss local time (SD) effects. The SC for the first storm occurred at 00:29 LT on 9 April and the enhancement in N_T occurred during the broad minimum usually found near dawn. The second SC occurred at 07:43 LT on the 14th and the positive phase maximum in N_T occurred near local noon. Thus, in both cases the time-lag from SC to $\Delta N_T(\max)$ was 3 to 5 hours. Figure 8-4c gives an example of some nighttime increases in N_T during a period when no storm SC was reported but when global conditions were generally disturbed. During the 6 hour period countered on 00 UT of 22 April, K_p was 6^+ and 5^- . We agree with the suggestions made by Rai and Hook (1967) and Bradbury et al (1968) that the precipitation of low energy electrons is the probable cause of nighttime enhancements in TEC at auroral latitudes.

In order to present in the greatest detail available a few examples of the diurnal N_T curves measured from Thule, we have prepared in Figure 8-5 tracings of the actual polarimeter data taken on 14 April ($A_p = 39$, $\sum K_p = 28^+$) and on 25 April ($A_p = 1$, $\sum K_p = 2^-$). The storm effects on the 14th are quite dramatic, while the extremely calm (geomagnetically) day closely follows the monthly median curve in Figure 8-3. It is interesting to note that even on a quiet day a certain amount of variability is apparent.

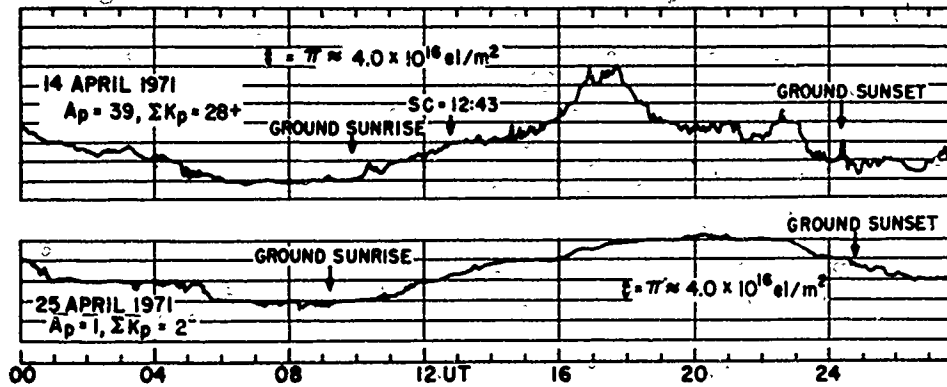


Figure 8-5. ATS-3 From Thule, Greenland, 14 and 25 April 1971.
 (76.6°N, 68.7°W), Sub-Ionospheric Point (400 km) = 61.6°N, 75.1°W, $\Lambda = 73^\circ$,
 Elevation to ATS-3 = 4.6°

8.4. DISCUSSION

Perhaps the three most prominent features evident in this preliminary set of data are

- (1) the solar zenith angle influence in the diurnal variation,
- (2) the definite response noted to geomagnetic storms, and
- (3) the irregular fluctuations found at all times, especially the nighttime hours.

There are at the present time no published reports of the complete diurnal N_T behavior at high latitudes with which these results may be compared. However, for several years Litzka's group in Sweden and Frihagen's group in Norway have used low-orbit data to extensively study total content at high latitudes. The Norwegian results include a particularly interesting set of data from Kjeller (60 deg North, 11 deg East) and Spitzbergen (78 deg North, 14 deg East). N_T data obtained from the 40 and 41 MHz beacons on the satellite S-66 as seen from Kjeller refer to approximately the same geographic latitude (60 deg) as the present Thule data, while S-66 passes taken near 76 deg from Spitzbergen yield N_T data at approximately the same L-shell as the Thule data. At middle and low latitudes (that is, within the plasmasphere) the geomagnetic field plays such a dominating role in determining the distribution of ionospheric plasma that one normally thinks in terms of comparing data from two stations which have the same geomagnetic coordinates. The data taken from Thule, however, measures electrons situated well above the plasmapause (that is, north of the main trough) and thus it is not clear whether geomagnetic or geographic (solar) control has the greatest influence. Bratteng and Frihagen (1969) presented some Spitzbergen data taken during the Spring of 1966

which seems to indicate that the overall diurnal range at 76 deg was less than the range reported at Kjeller (60 deg) for the Spring of 1965 [Frihagen and Bratteng (1967)]. Considering the April median in Figure 8-3 as well as feature (1) noted above, it appears that the solar zenith angle control exerts the dominant influence over the diurnal N_T variation measured from Thule.

In conclusion, we wish to say that while emphasis has been placed on the solar control over the TEC results reported here, the corpuscular sources of ionization are certainly important. This was briefly discussed in connection with Figure 8-4 c and it appears that particle influence may also be evident in Figure 8-2. Near 1500 LT in this figure, there seems to be an avoidance of low N_T values. This time period corresponds to approximately 2000 UT, the same UT period when a maximum in the soft electron precipitation is expected [see Maehlum, (1968) and Pike, (1970)]. Bratteng and Brihagen (1969) reported similar effects during winter months when the possibility of observing a UT variation is the greatest. Such effects will be examined in more detail as soon as our Winter data becomes available.

References

- Bratteng, O.M. and Frihagen, J. (1969) The Electron Content in the Polar F Region, Scientific Report No. 2 of EOAR Contract No. F61062-67-C-0020.
- Bradbury, J.N., Evans, J.E., Joki, E.G., Moe, C.R., and Hook, J.L. (1968) Simultaneous measurements of electron content and charged-particle precipitation in a region of auroral activity, J. Geophys. Res. 73:2363.
- Chan, K.L. and Colin, L. (1969) Global electron density distributions from topside sounding Proc. IEEE, 57:990.
- Frihagen, J., and Bratteng, O.M. (1967) Total Electron Content Measurements at High Altitudes. Final Scientific Report, AF61(052)-860.
- Garriott, O.K., daRosa, A.V. and Ross, W.J. (1970) Electron content obtained from Faraday rotation and phase path length variations, J. Atmos. Terr. Phys. 32:705.
- Hibberd, F.H., and Ross, W.J., Variations in total electron content and other ionospheric parameters associated with magnetic storms, J. Geophys. Res., 72:5331.
- Liszka, L. (1966) Latitudinal and diurnal variations of the ionospheric electron content near the auroral zone in winter, Radio Science, 1:1135.
- Maehlum, B.N. (1968) Universal time control of the low-energy electron fluxes in the polar regions, J. Geophys. Res. 73:3459.
- Mendillo, M. (1971) Ionospheric total electron content behavior during geomagnetic storms, submitted to Nature.
- Pike, C.P. (1971) University time control of the south polar F layer during the IGY, J. Geophys. Res. 75:4871.
- Rai, D.B., and Hook, J.L. (1967) Total electron content and its variations in the auroral zone ionosphere during winter, J. Geophys. Res. 72:5319.

Contents		
9-1	Methods Used, Problems and Limitations in Obtaining TEC Data	61
9-2	TIDs-A Limiting Factor in Obtaining True TEC Value	62
9-3	Improving Prediction Accuracy	63

9. Conclusions

J.A. Klobuchar

9.1. METHODS USED, PROBLEMS AND LIMITATIONS IN OBTAINING TEC DATA

The present state of the art of TEC values for use in time delay corrections for systems applications is a mixed bag. In this report we have outlined several existing models from which a TEC value may be obtained. We have tried to avoid comparisons among these models as they have not been adequately and uniformly tested against real data in any comparative way. Our emphasis here has been to present data from the three, more or less, naturally defined world regions, namely the equatorial, mid-latitude and polar regions. In one case sufficient average data were available to construct a model of TEC which is of use in the European sector in a limited way. Also, the statistics of TEC variability were given in the data section for a mid-latitude station. Many maps of TEC iso-contours also were shown, particularly for the European sector. Any one or a combination of the above models and/or data sets should serve as a first order TEC time delay correction source.

Several problems and limitations in TEC data were discussed and more problems will be addressed briefly here. The basic problems are:

- (1) the lack of complete measurements of the many variables responsible for the behavior of the electron density in the ionosphere; and
- (2) the lack of sufficient experimental data to produce an empirical ionospheric electron density model of sufficient accuracy.

Since the approach in (1) follows from first principles it is the more elegant, but also far from complete, solution. Hence, an empirical model of the parameter of direct interest is the alternate approach, and all empirical ionospheric models are data-base limited.

The specific TEC data base limitations, aside from the obvious one of lack of data from a particular geographic region, are several. TEC from low orbit satellites is inadequate because it can only determine TEC up to the satellite height of approximately 1000 km, and then only when the satellite is sufficiently above the station's horizon, which may be only for four to six 10-minute periods per day. During times of heavy amplitude scintillation, the Faraday fading is obscured and often unreadable. This happens particularly during magnetic storms when the TEC is probably most interesting to study, as during disturbed periods the TEC departure from median conditions are usually largest. Because of the motion of the satellite, changes in its beacon signal's transmitted polarization, and the changes in the mean height of the ionosphere, the estimated accuracy of TEC data obtained from low orbit satellites is not better than ± 10 percent. Due to the limited time sampling of TEC from low orbit satellites, only seasonal average data can usually be obtained.

Continuous temporal coverage is possible with TEC data derived from VHF beacon signals transmitted from geostationary satellites. No loss of data occurs during periods of severe amplitude scintillation if a good polarization follower (polarimeter) is used. However, with the Faraday method of TEC data determination, the TEC is measured only up to a vertical height of approximately 2000 to 3000 km, depending on the density at those heights. The TEC between 2000 to 3000 km and the satellite height of 36,000 km can equal the density below this height, at least at nighttime, and can be 10 to 20 percent of the complete total in the daytime. The estimated accuracy of determining TEC in the lower 2000 to 3000 km by the Faraday technique, from VHF signals transmitted from geostationary satellites, is plus and minus 5 percent.

9.2. TIDs - A LIMITING FACTOR IN OBTAINING TRUE TEC VALUE

Even if a true group path delay measurement of negligible error was made, along one direction from a particular station, a TEC model will still be required to correct that true TEC value for use along another slant direction from the same station. It is likely that such a model would be able to correct for the normal temporal and geographic variations in TEC. However, the limiting factor is the existence of small scale travelling ionospheric disturbances (TIDs) which can be of a size smaller than the distance in the ionosphere between the two slant directions viewed from a single station. The occurrence, size and location of a specific small scale TID cannot be predicted. Hence, these TIDs, which are typically from 1 to 5 percent of the TEC, may become the ultimate limitation to TEC corrections.

Ionospheric models which are required to independently correct for time delay with a resultant 50 percent rms error are relatively simple and are at hand. Three of the TEC models outlined in this report have been tested against TEC data, and, in the mid-latitudes, have obtained an approximate 75 percent rms ionospheric correction. However, a system which requires an independent correction for 99 percent (rms) of the ionospheric time delay had better not be built! A 50 percent rms correction is easy to accomplish in most cases; 99 percent is impossible; the task of ionospheric workers in this field is to get as close to 99 percent as is practical, in the most efficient way.

9.3. IMPROVING PREDICTION ACCURACY

The work which should greatly improve prediction accuracy involves the times when the greatest differences from median conditions occur. These times are usually, but not always, during magnetically disturbed conditions. An understanding of the physical mechanisms which produce the observed changes in TEC during magnetic storms is a long sought after goal; but, unfortunately, there is not yet even a completely clear experimental picture of the changes which occur in TEC on a statistical basis during magnetic storms over all regions of the earth. As more data are being collected a clearer picture will emerge and there is reason to believe that within a very few years a much better understanding of the world-wide behavior of total electron content will emerge.